ANGELHY

Innovative solutions for design and strengthening of telecommunications and transmission lattice towers using large angles from high strength steel and hybrid techniques of angles with FRP strips

WORK PACKAGE 1 – DELIVERABLE 1.3

Report on analysis and design of 6 case studies

Coordinator:

National Technical University of Athens - NTUA, Greece

Beneficiaries:

ArcelorMittal Belval & Differdange SA - AMBD, Luxembourg

Universite de Liege - ULG, Belgium

COSMOTE Kinites Tilepikoinonies AE - COSMOTE, Greece

Centre Technique Industriel de la Construction Metallique - CTICM, France

SIKA France SAS - SIKA, France

AUTHORS:

COSMOTE Kinites Tilepikoinonies AE - COSMOTE, Greece

19002 Paiania, Greece

Authors: Aggeliki Papailiopoulou, Michael Papavasileiou, Theodoros Bessas

NATIONAL TECHNICAL UNIVERSITY OF ATHENS

Institute of Steel Structures

15780 Athens, Greece

Authors: Ioannis Vayas, Pavlos Thanopoulos, Dimitrios Vamvatsikos, Konstantinos Vlachakis, Maria-Eleni Dasiou

ARCELORMITTAL BELVAL&DIFFERDANGE SA

Global R&D

66, rue de Luxembourg

L-4009 Esch-sur-Alzette, Luxembourg

Authors: Mike Tibolt

UNIVERSITE DE LIEGE

Faculty of Applied Sciences, ArGEnCo Department

Quartier Polytech 1, Allée de la Découverte, 9, B52/3, 4000 Liège, Belgium

Authors: Marios-Zois Bezas, Jean-Pierre Jaspart, Jean-François Demonçeau

CENTRE TECHNIQUE INDUSTRIEL DE LA CONSTRUCTION METALLIQUE - CTICM
Steel Construction Research Division
Espace Technologique – Immeuble Apollo
L'Orme des Merisiers – F-91193 Saint Aubin
Authors: André Beyer, Alain Bureau

TABLE OF CONTENTS

1   Telecommunication towers

1.1   Introduction

In the current report the assessment study of an existing self-supporting lattice tower of the Cosmote telecommunication network is presented. Initially an assessment of the existing tower is carried out without any ancillaries in order to evaluate the bearing capacity of the structure itself according to the current Codes. Subsequently, two strengthening alternatives are evaluated and compared. In the first 'conventional' method, the diagonal and horizontal members are replaced with larger sections and the legs are strengthened by connecting an equal L-section to the existing one so that a star battened angle member is created. In the second alternative, the tower members are strengthened by FRP's as required.

For the study, the geometry of the structure is taken from the shop drawings provided by the telecommunication company.

Further on, it is assumed that no corrosion or other adverse effect has altered the geometry or the mechanical characteristics of the material of the members.

1.2   Design specifications

The following design codes and standards are used for the structural analysis and design:

[1]   EUROCODE 1: Actions on structures – Part 1-4: General actions- Wind actions

[2]   EUROCODE 3: Design of steel structures – Part 1-1: General rules and rules for buildings.

[3]   EUROCODE 3: Design of steel structures – Part 3-1: Towers, masts and chimneys – Towers and masts

[4]   EUROCODE 8: Design of structures for earthquake resistance - General rules, seismic actions and rules for buildings

1.3   Materials

The Steel grade of the structural members is S235 according to EN 10025. The material's properties used for the structural analysis and design are shown in Table 1.1 and Figure 1.1 . The safety factor for the material is taken as $\gamma_m = 1.10$.

Table 1.1: Material's properties

Mat 1 S 235 (EN 1993)

Young's modulus	E	210000	[N/mm2]	Safetyfactor		1.10	[-]
Poisson's ratio	μ	0.30	[-]	Yield stress	fy	235.00	[MPa]
Shear modulus	G	80770	[N/mm2]	Compressive yield	fyc	235.00	[MPa]
Compression modulus	K	175000	[N/mm2]	Tensile strength	ft	360.00	[MPa]
Weight	γ	78.5	[kN/m3]	Compressive strength	fc	360.00	[MPa]
Density	ρ	7850.00	[kg/m3]	Ultimate strain		100.00	[o/oo]
Elongation coefficient	α	1.20E-05	[1/K]	relative bond coeff.		0.00	[-]
max. thickness	t-max	40.00	[mm]	EN 1992 bond coeff.	k1	0.00	[-]
				Hardening modulus	Eh	0.00	[MPa]
				Proportional limit	fp	235.00	[MPa]
				Dynamic allowance	σ-dyn	0.00	[MPa]

S 235 (EN 1993)
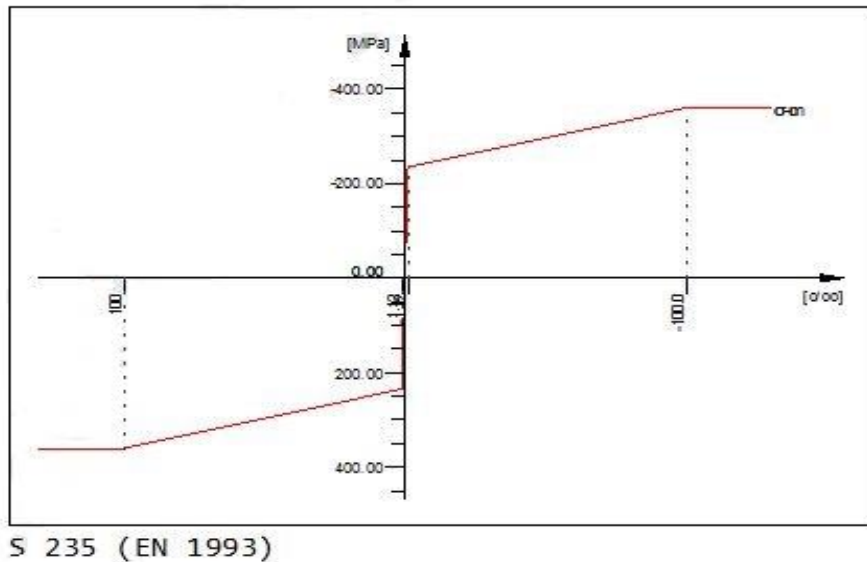
Figure 1.1: Material's stress-strain curve

1.4 Loads

For the study of the lattice towers, the following permanent and variable loads are taken into account:

1.4.1 Permanent Loads

- **Self-weight of steel structure**

The self-weight is calculated by the analysis program considering the specific weight of steel γ=78.50 kN/m^3

- **Weight of climbing ladder, waveguide rack and cables, lightning rod**

The weight of the climbing ladder is equal to 0.153 kN/m. The weight of the waveguide rack is equal to 0.146 kN/m.

In addition, a lightning rod Φ48.3*3.2 with length of 1.25 m and a weight of 0,045kN is taken into account, placed on the top of the tower.

- **Self-weight of working platforms**

Working platforms are located at +12.00, +24.00, +36.00, +42.00 and +45.00m height. The weight of each platform is equal to 0.235kN/m^2.

1.4.2 Live Loads

- **Live Load of climbing ladder**

The live load of the climbing ladder has been taken equal to **1 kN/m** .

- **Live Load of working platforms**

The live load of the working platforms has been taken equal to **2 kN/m² .**

1.4.3 Ice load

For the calculation of ice load, it is assumed that all structural members, components of ladders, ancillaries etc are covered with ice having a thickness of 30mm over the whole surface of the member. (Ice density has been taken equal to 7.00 kN/m³). Thus, i.e. the ice load for the parabolic antennas is calculated based on the following formula:

$$G_S = \frac{\pi \times a}{2} \times \left[2 \times b \times (\Phi + a) + (\Phi + 2 \times a)^2\right] \times \gamma_{ice} \quad , [kN]$$ **Eq. 1.1**

a b a
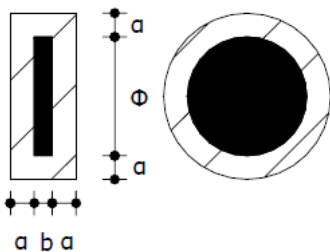
1.4.4 Wind

Based on Eurocode 1 and the Greek National Annex the basic wind speed for the study is taken equal to 33m/sec, since the structure is located in an area with distance from the sea smaller than 10km.

'Gust' wind load

The gust wind force acting on the incremental area j of the structure at the height z_j is determined from:

$$F_{t,w}(z_i) = F_{m,w}(z_i) \left(1 + \frac{1 + 0.2\left(\frac{z_i}{h}\right)^2}{c_o(z_i)} \left[(1 + 7I_v(z_i))c_s c_d - 1\right] \right)$$ **Eq. 1.2**

where:

$F_{m,w}$ is the mean wind load force

$c_s c_d$ is the structural factor, taken as 1.

z_j height of the center of gravity of incremental area A_j

$I_v(z_i)$ turbulence intensity at height z_i

$c_0(z_i)$ orography coefficient at height z_i

Mean wind load

The mean wind force acting on the structure is determined from a summation of pressures acting on surfaces. The mean force F_{wj} acting on the incremental area j at the height z_j is:

$$F_{m,w}(z_i) = \frac{q_p}{1+7I_V(z_i)} \sum c_f A_{rcf}$$

Eq. 1.3

where:

  q_P is the basic velocity pressure

  c_f force coefficient for incremental area A_j

  z_j height of the centre of gravity of incremental area A_j

  A_{ref} Reference area

  $I_v(z_i)$ turbulence intensity at height z_i

The basic velocity pressure at the height z_j is:

$$q_p(z_i) = [1+7 \cdot I_v(z_i)] \cdot \frac{1}{2} \cdot \rho \cdot v_m^2(z_i)$$

Eq. 1.4

where:

  v_m is the mean wind velocity

  ρ is the air density (equal to $1.25 Kg/m^3$)

  z_j height of the center of gravity of incremental area A_j

  $I_v(z_i)$ turbulence intensity at height z_i

The mean wind velocity at the height z_j is:

$$v_m(z_i) = c_r(z_i) \cdot c_o(z_i) \cdot v_b$$

Eq. 1.5

where:

  v_b is the basic wind velocity

  $c_r(z)$ is the roughness coefficient

  $c_o(z)$ is the orography coefficient

  z_j height of the center of gravity of incremental area A_j

The basic wind velocity, defined as a function of wind direction and time of year at 10m above ground of terrain category II, is:

$$v_b = c_{dir} \cdot c_{season} \cdot v_{b,0}$$

Eq. 1.6

where:

  $v_{b,0}$ is the fundamental value of the basic wind velocity, taken as **33.00m/sec**.

  c_{dir} is the directional factor, taken as 1.

  c_{season} is the season factor, taken as 1.

Due to symmetry, two wind directions, 0^0 (W_o) and 45^0 (W_l) were considered. For the two wind directions, the total wind load is distributed on each side of the tower according to Table 1.2:

Table 1.2: Table of wind rates to the surface

		I	II	III	IV
	W_o vertical to surface	57%	0%	43%	0%
	W_o pararell to surface	0%	0%	0%	0%
	W_l vertical to surface	20%	20%	15%	15%
	W_l pararell to surface	20%	20%	15%	15%

1.4.5 Earthquake

The earthquake loading is calculated in accordance with Eurocode 8. For the modal analysis the following parameters have been taken into account:
  – Peak ground acceleration, a = 0.24g
  – Importance factor, γ = 1.40
  – Behavior factor, q = 1.00
  – Soil class B
  – Modal damping 4%

1.5 Global analysis and load combinations

Global analysis was performed by application of the SOFISTIK software. All structural members are simulated as by means of 6DOF beam elements. Hinges are assigned to the ends of all horizontal and diagonal members, as well as at the column bases. Linear elastic 1st order analysis was performed.

Based on Eurocode 3 Part 3-1 for the assessment of a lattice tower, following load combinations are considered for the cross-section and member checks of the legs:

1. $1.00 \cdot G + 1.20 \cdot Q$
2. $1.00 \cdot G + 1.20 \cdot Q + 0.60 \cdot 1.20 \cdot W_G$
3. $1.00 \cdot G + 1.20 \cdot Q + 0.60 \cdot 1.20 \cdot W_{GS} + 0.70 \cdot 0.50 \cdot 1.20 \cdot S$
4. $1.00 \cdot G + 1.20 \cdot W_G + 0.70 \cdot 1.20 \cdot Q$
5. $1.00 \cdot G + 0.64 \cdot 1.20 \cdot W_{GS} + 0.5 \cdot 1.20 \cdot S + 0.70 \cdot 1.20 \cdot Q$
6. $G + 0.30 \cdot S + 0.30 \cdot Q \pm E$

For all the other members (diagonals, horizontals, etc), following load combinations have been taken into account for the cross-section and member checks:

1. $1.00 \cdot G + 1.20 \cdot Q$
2. $1.00 \cdot G + 1.20 \cdot Q + 0.60 \cdot 1.20 \cdot W_{O,G}$
3. $1.00 \cdot G + 1.20 \cdot Q + 0.60 \cdot 1.20 \cdot W_{G,O}$
4. $1.00 \cdot G + 1.20 \cdot Q + 0.60 \cdot 1.20 \cdot W_{O,G,S} + 0.70 \cdot 0.5 \cdot 1.20 \cdot S$

5. $1.00 \cdot G + 1.20 \cdot Q + 0.60 \cdot 1.20 \cdot W_{G,O,S} + 0.70 \cdot 0.5 \cdot 1.20 \cdot S$
6. $1.00 \cdot G + 1.20 \cdot W_{O,G} + 0.70 \cdot 1.20 \cdot Q$
7. $1.00 \cdot G + 1.20 \cdot W_{G,O} + 0.70 \cdot 1.20 \cdot Q$
8. $1.00 \cdot G + 0.64 \cdot 1.20 \cdot W_{O,G,S} + 0.5 \cdot 1.20 \cdot S + 0.70 \cdot 1.20 \cdot Q$
9. $1.00 \cdot G + 0.64 \cdot 1.20 \cdot W_{G,O,S} + 0.5 \cdot 1.20 \cdot S + 0.70 \cdot 1.20 \cdot Q$
10. $G + 0.3 \cdot S + 0.3 \cdot Q \pm E$

where:
   a) W is the wind without ice
   b) Ws the wind with ice.
   c) W_G is the wind with gust
   ~~d)~~ $W_{O,G}$ is the wind with gust of the lower part of the tower
   e) $W_{G,O}$ is the wind with gust of the upper part of the tower
   f) For the combination of wind with ice, the wind load Ws is multiplied with the factor ks = 0.64

1.6 Initial tower

1.6.1 General

This paragraph concerns the design of the initial tower. Loads and load combinations are adopted from the previous paragraphs 1.4 and 1.5.

The geometrical properties of this tower are indicated in Figure 1.2. The tower is built by 6.00m long similar pyramidal and rectangular bodies, easy to be assembled, has anti-climb platform and anti-climb protection door at 3.00m high above the ground. The lattice tower consists of two sections. The first section is an inclined one of 24.00m height, with plan dimensions starting from 5.55m to 2.50m. The second section is the vertical part of the tower that the antennas are placed, therefore for practical reasons has no inclination.
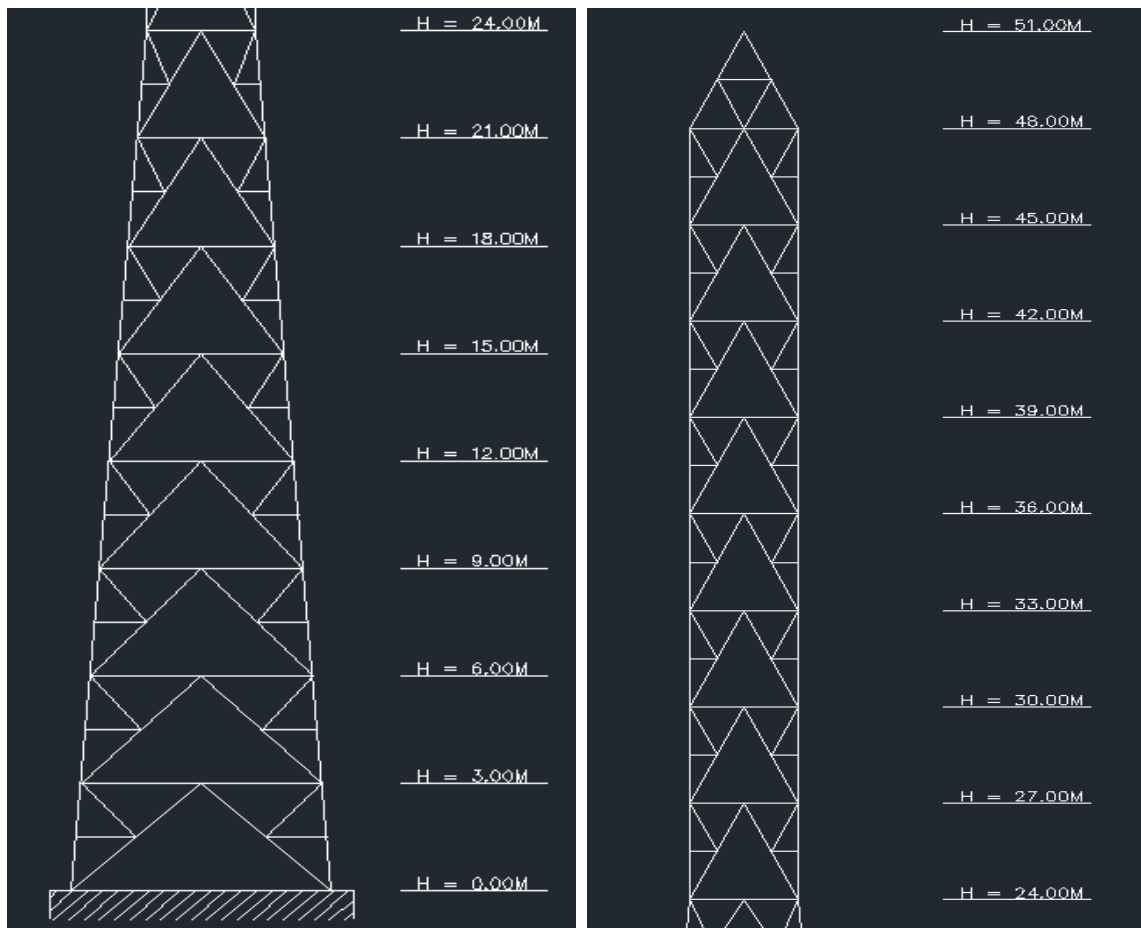
Figure 1.2: Lattice Tower

Secondary horizontal angle members are also placed in order to reduce the buckling length of the main horizontal members and to carry the waveguide rack and the climbing ladder. The vertical diagonal braces form a Λ type with additional angle members that reduce the buckling length in both directions of the braces.
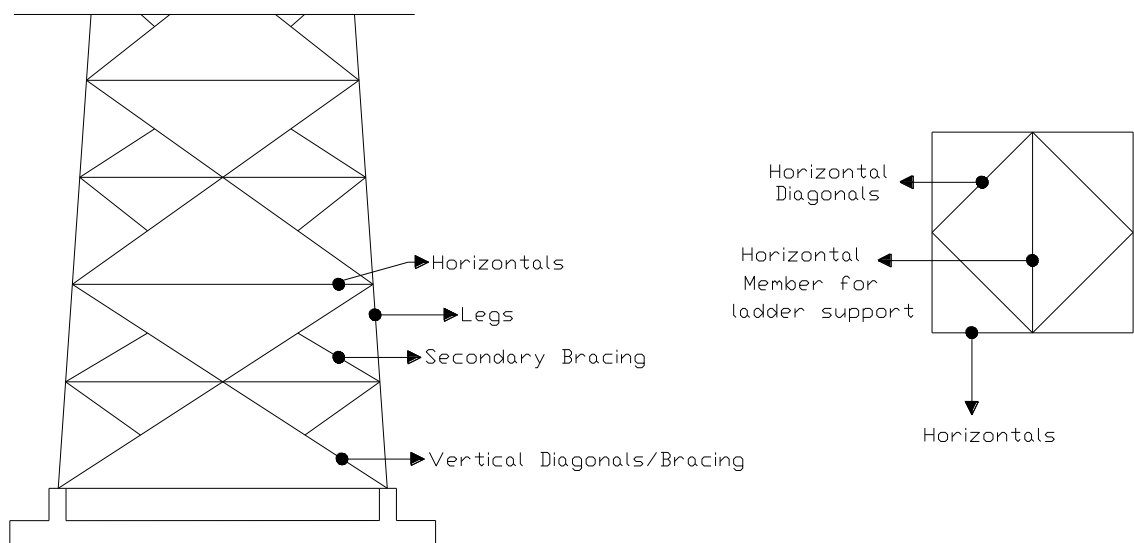
Figure 1.3: Designation of structural members

The cross sections and the diaphragm of the structural system is shown in Table 1.3:

Table 1.3 : Cross sections of the tower

No		Type of member	Section
1		Legs at height 0 – 24 m	L160.15
2		Legs at height 24 – 48 m	L120.12
4		Vertical bracing system and members at the top of the tower	L70.7
5		Secondary vertical bracing system and horizontal bracing system (except from levels with resting platforms)	L45.5
6		Horizontal bracing system at levels with resting platforms (heights 12, 24, 36, 42, 45 m)	U80
7		Horizontal members	U100
8		Central Horizontal members These members bear the loads of the ladder, the waveguide rack and the cables	2 x U160 welded on both edges

1.6.2 Structural design

Global analysis was followed by structural design, where all members are checked in accordance with EN 1993-1-1 and EN 1993-3-1 using the software package SOFISTIK-STEEL MEMBERS.

Table 1.4 is an excerpt of the design results for the tower legs indicating the utilization factor against flexural buckling to compression and bending (FLB), lateral torsional buckling (LTB) and buckling to pure compression (buckl). The utilization factor for full exploitation of the cross-section is 1.0 (100%). Larger values indicate no permissible overloading of members.

Table 1.4: Table of rates for the towers legs

Beam	LC	Class	Mv	Mz	Qv	Qz	N	(N+M+V)		LTB	Buck.	BAT
									Legs of the tower			
1	max ***	3	0.12	0.12	0.01	0.01	1.08	1.21	1.58		1.31	
2	max ***	3	0.14	0.14	0.01	0.01	1.08	1.2	1.47		1.31	
3	max ***	3	0.15	0.15	0.01	0.01	1.03	1.2	1.46		1.23	
4	max ***	3	0.15	0.15	0.01	0.01	1.03	1.21	1.45		1.23	
5	max ***	3	0.16	0.16	0.01	0.01	0.98	1.18	1.41		1.17	
6	max ***	3	0.16	0.16	0.01	0.01	0.98	1.18	1.41		1.17	
7	max ***	3	0.16	0.17	0.01	0.01	0.92	1.13	1.35		1.1	
8	max ***	3	0.16	0.17	0.01	0.01	0.92	1.14	1.35		1.1	
9	max ***	3	0.17	0.18	0.02	0.02	0.86	1.1	1.31		1.03	
10	max ***	3	0.17	0.18	0.02	0.02	0.86	1.1	1.3		1.03	
11	max ***	3	0.19	0.19	0.02	0.02	0.81	1.08	1.27		0.97	
12	max ***	3	0.19	0.19	0.02	0.02	0.81	1.08	1.27		0.97	
13	max ***	3	0.2	0.2	0.02	0.02	0.76	1.06	1.24		0.91	
14	max ***	3	0.2	0.2	0.02	0.02	0.77	1.06	1.23		0.92	
15	max ***	3	0.19	0.2	0.02	0.02	0.72	1.01	1.17		0.86	
16	max ***	3	0.19	0.2	0.01	0.01	0.72	1.01	1.23		0.86	
17	max ***	3	0.42	0.17	0.01	0.02	0.94	1.3	1.71		1.29	
18	max ***	3	0.42	0.27	0.02	0.02	0.94	1.3	1.71		1.29	
19	max ***	3	0.3	0.27	0.02	0.02	0.71	1	1.25		0.97	
20	max ***	3	0.3	0.22	0.01	0.02	0.71	1	1.2		0.97	
21	max	3	0.2	0.22	0.01	0.01	0.51	0.7	0.91		0.7	
22	max	3	0.2	0.17	0.01	0.01	0.51	0.7	0.94		0.7	
23	max	3	0.12	0.17	0.01	0.01	0.34	0.45	0.59		0.47	
24	max	3	0.12	0.13	0.01	0.01	0.34	0.45	0.61		0.47	
25	max	3	0.07	0.13	0.01	0.01	0.21	0.28	0.36		0.29	0
26	max	3	0.06	0.09	0.01	0	0.21	0.26	0.36		0.28	0
27	max	3	0.03	0.09	0.01	0	0.11	0.16	0.2		0.14	0
28	max	3	0.03	0.06	0.01	0	0.1	0.13	0.17		0.14	0
29	max	3	0.03	0.06	0.01	0	0.04	0.07	0.08		0.05	0
30	max	3	0.02	0.03	0	0	0.04	0.05	0.07		0.05	0
31	max	3	0.02	0.03	0	0	0.01	0.03	0.04		0.01	
32	max	3	0.02	0.02	0	0	0.01	0.02	0.03		0.01	
33	max	3	0.04	0.04	0	0	0.01	0.06	0.08		0.03	0
34	max	3	0.04	0.04	0	0	0	0.06	0.07		0.01	0
101	max ***	3	0.12	0.12	0.01	0.01	1.08	1.21	1.58		1.31	
102	max ***	3	0.14	0.14	0.01	0.01	1.08	1.21	1.47		1.31	
103	max ***	3	0.15	0.15	0.01	0.01	1.03	1.21	1.46		1.23	
104	max ***	3	0.15	0.15	0.01	0.01	1.03	1.21	1.45		1.23	
105	max ***	3	0.16	0.16	0.01	0.01	0.98	1.18	1.41		1.17	

The exploitation rate of more than 1.0 of one member, suggests "failure", which means that the mentioned member do not cover the required regulations regarding the safety of the structure. Rates less than 1.0 suggest that the member could receive more stress.

Eventually, we can conclude that the first and the second category (legs, vertical diagonal members) have exceeded the limits of max safety margins.

In Table 1.5 the maximum utilization factors are given for each member type of the tower.

Table 1.5: Maximum utilization factor for each member type

Member type	Maximum utilization factor	Overloading in segments
Legs	1.89	0-33m
Vertical diagonals	1.59	0-12m and 24-36m
Horizontals	0.45	
Secondary bracing members	0.63	
Horizontal diagonal members	0.96	
Members supporting climbing ladder	0.31	

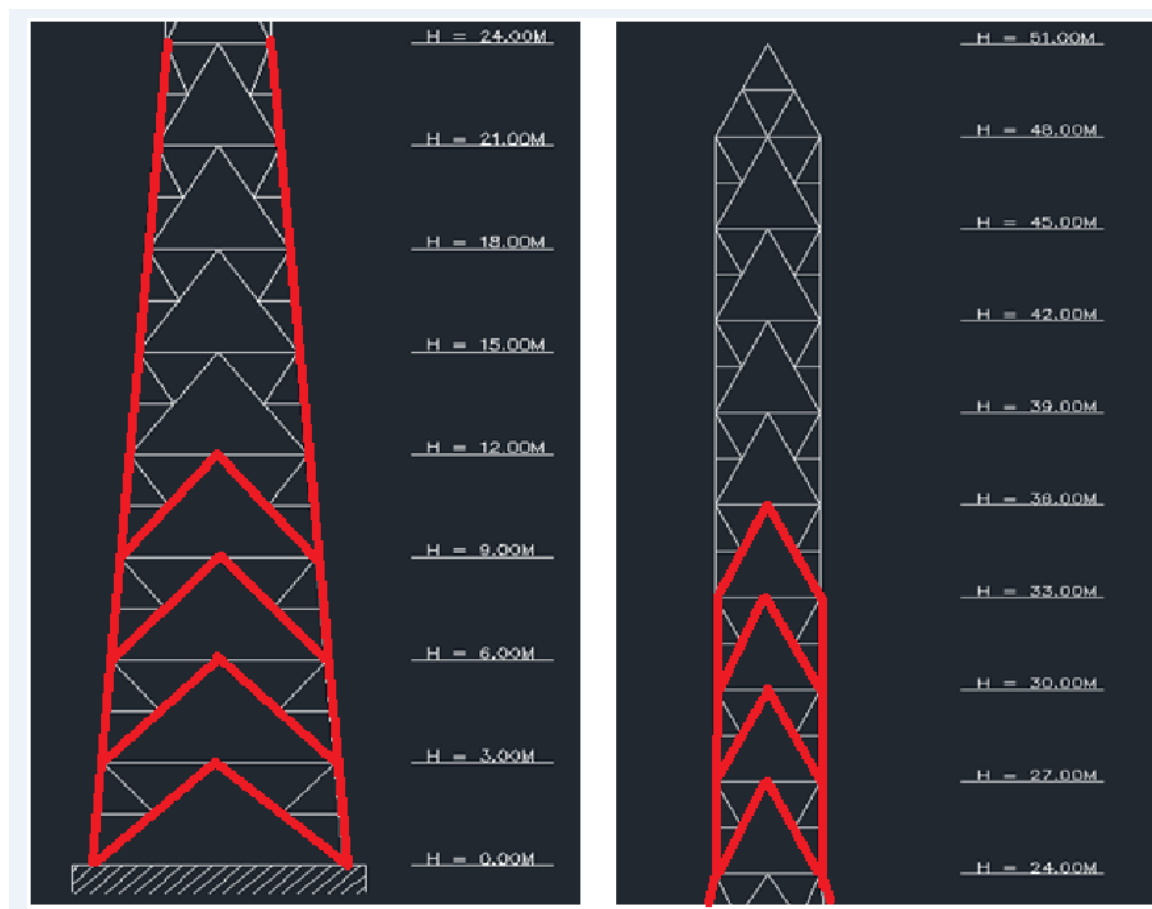In Figure 1.4 the members designated with red are exceeding the allowable stress and need strengthening.

Figure 1.4: Members designated with red are exceeding the allowable stress and need strengthening

1.7   Conventionally strengthened tower

1.7.1   General

In paragraph 1.6 the assessment of an existing self-supporting lattice tower without any ancillaries was presented. As indicated in paragraph 1.6.2 several members, mainly legs and diagonal, exceed their capacity. Thus, strengthening of the tower is necessary. In the current paragraph a 'conventional' strengthening method is examined, where the structural members that exhibit 'failure' are either replaced or reinforced.

In specific:

1. The legs are strengthened by connecting the existing L-section with an equal L-section so that a star battened angle member is created (see Figure 1.5)
2. The main vertical diagonal members are either replaced with members of larger L-sections or by connecting an equal L-section back to back to the existing L-section (see Figure 1.6)
3. The secondary vertical diagonal members are replaced with members of larger L-sections.
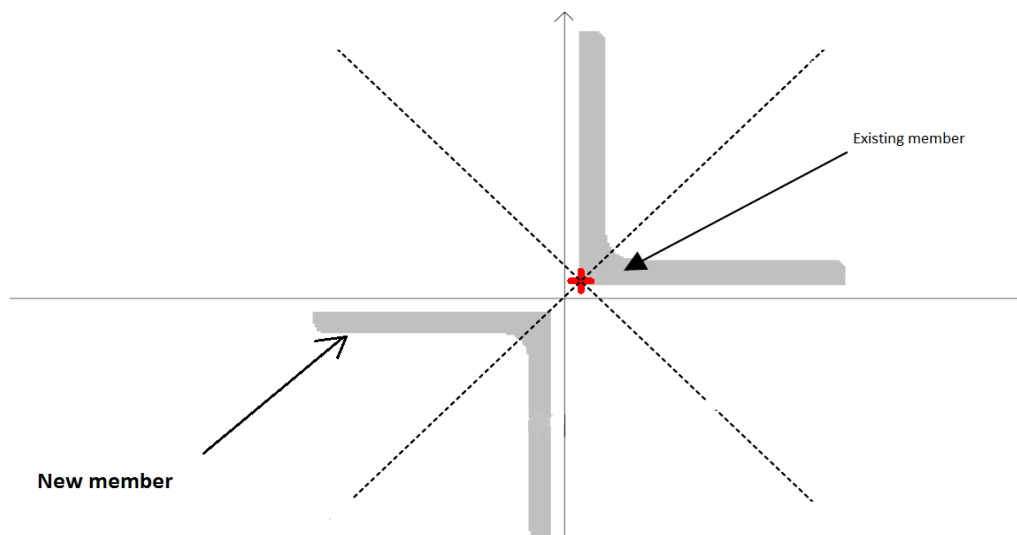

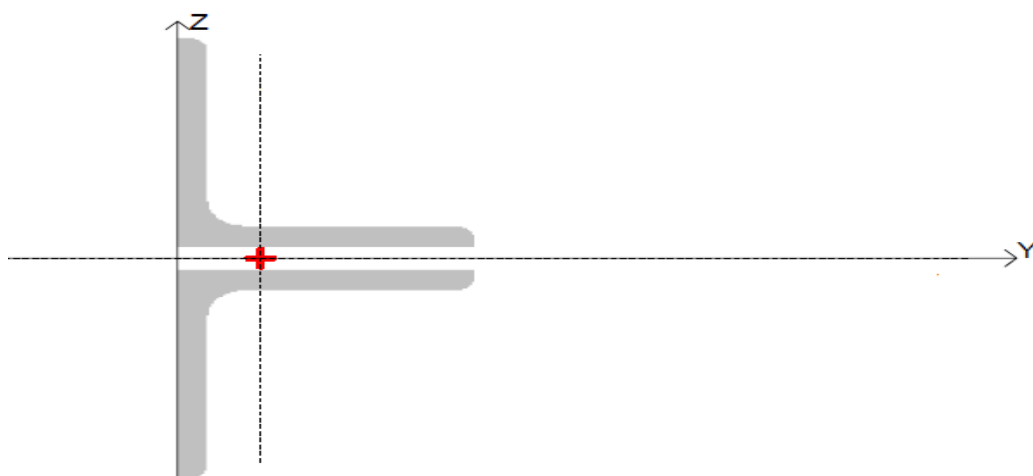**Figure 1.5: Strengthening of legs**

Figure 1.6: Strengthening of main vertical diagonal members by connecting a new equal L-section with the existing one.

In Table 1.6 the sections of each member type of the initial and the strengthened tower are given.

Table 1.6: Sections of the initial and strengthened tower for each member type

Members	Height	Exsisting members	New members
Legs	0-24m	L160.15	2L160.15/20
	24-33m	L120.12	2L120.12/20
Vertical diagonal	0-24m	L70.7	L80.8
	24-30m	L70.7	2L70.7/10
	30-42m	L70.7	L80.8
Secondary diagonal	12-18m	L45.5	L50.5
	18-24m	L45.5	L60.6
	24-30m	L45.5	L505

1.7.2 Design loads

General

Design loads are given in paragraph 1.4. In addition to those four parabolic antennas with a diameter of 2.40m are assumed on each side of the tower, at the top (height 45-48m).

Weight of parabolic antennas

The parabolic antennas are placed on the tower through a special designed system. The system is made of 12mm thick hot-dip galvanized steel plates with a length of 3.00m. The length of the support arms is 0.50m. Each antenna weighs 2.3 kN.
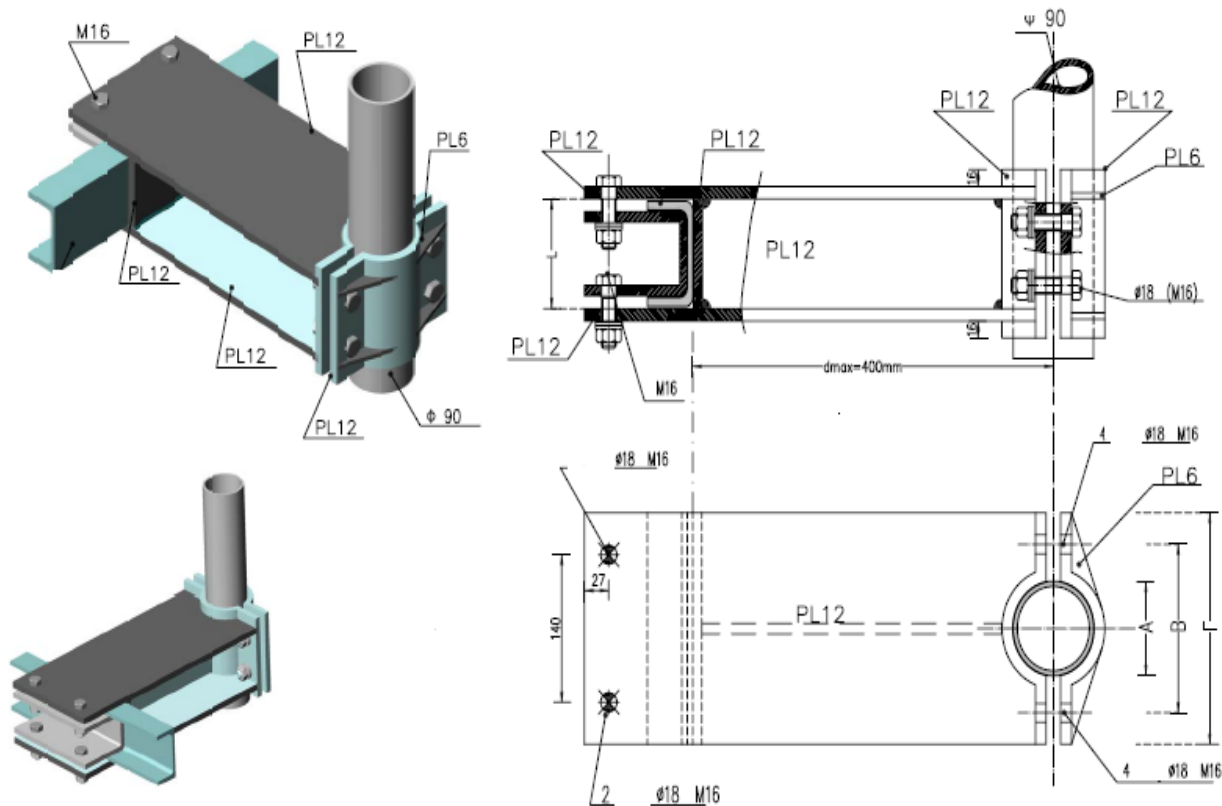

Figure 1.7: Antenna Support system placed at the horizontal UPN members of the tower

Figure 1.8: Antenna Support system placed at the horizontal double angle members of the tower

Figure 1.9: Position of parabolic antennas on tower

Wind Load on parabolic antennas

The wind load on the parabolic antennas is calculated with the use of the freeware software Andwind. Force (F_A) acts along the axis of the antenna, side force (F_S) acts perpendicular to the antenna axis and the twisting moment (M) acts in the plane containing F_A and F_S.
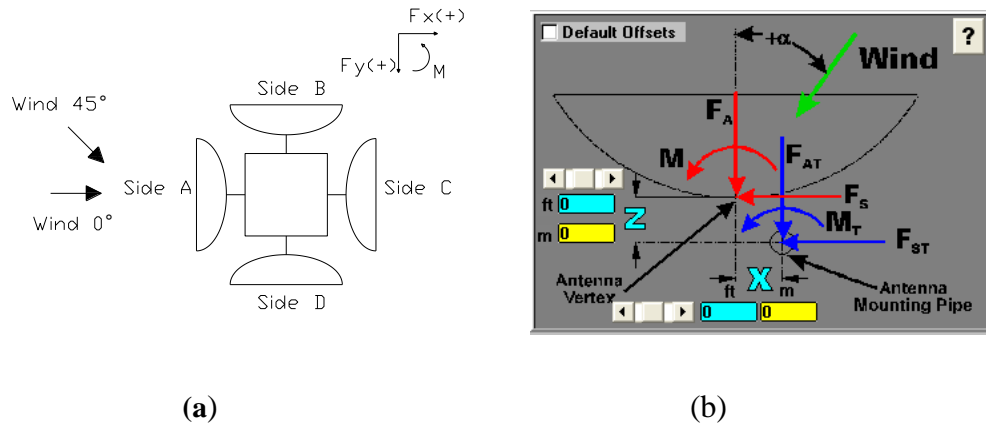

(a)   (b)

Figure 1.10: (a) Configuration of the parabolic antennas on the tower and (b) depiction of the wind forces acting on a parabolic antenna

The wind forces on a 2.40 m diameter parabolic antenna are given in Table 1.7.

Table 1.7: Wind forces for a 2.40 m diameter parabolic antenna located at 45m height

Side	Angle θ of the wind loading	F_a (kN)	F_s (kN)	Moment (kNm)
A	0º	9.060	0.000	0.000
	45º	8.050	2.104	-0.712
B	0º	4.490	-0.790	-1.720
	45º	2.104	8.050	0.712
C	0º	7.300	0.000	0.000
	45º	6.440	1.950	-1.500
D	0º	4.490	0.790	1.720
	45º	1.950	6.440	1.500

1.7.3 Structural design

In Figure 1.11 the members designated with red were strengthened. The members designated with green were strengthened in a star battened or back to back configuration, while the rest were replaced by larger angles.
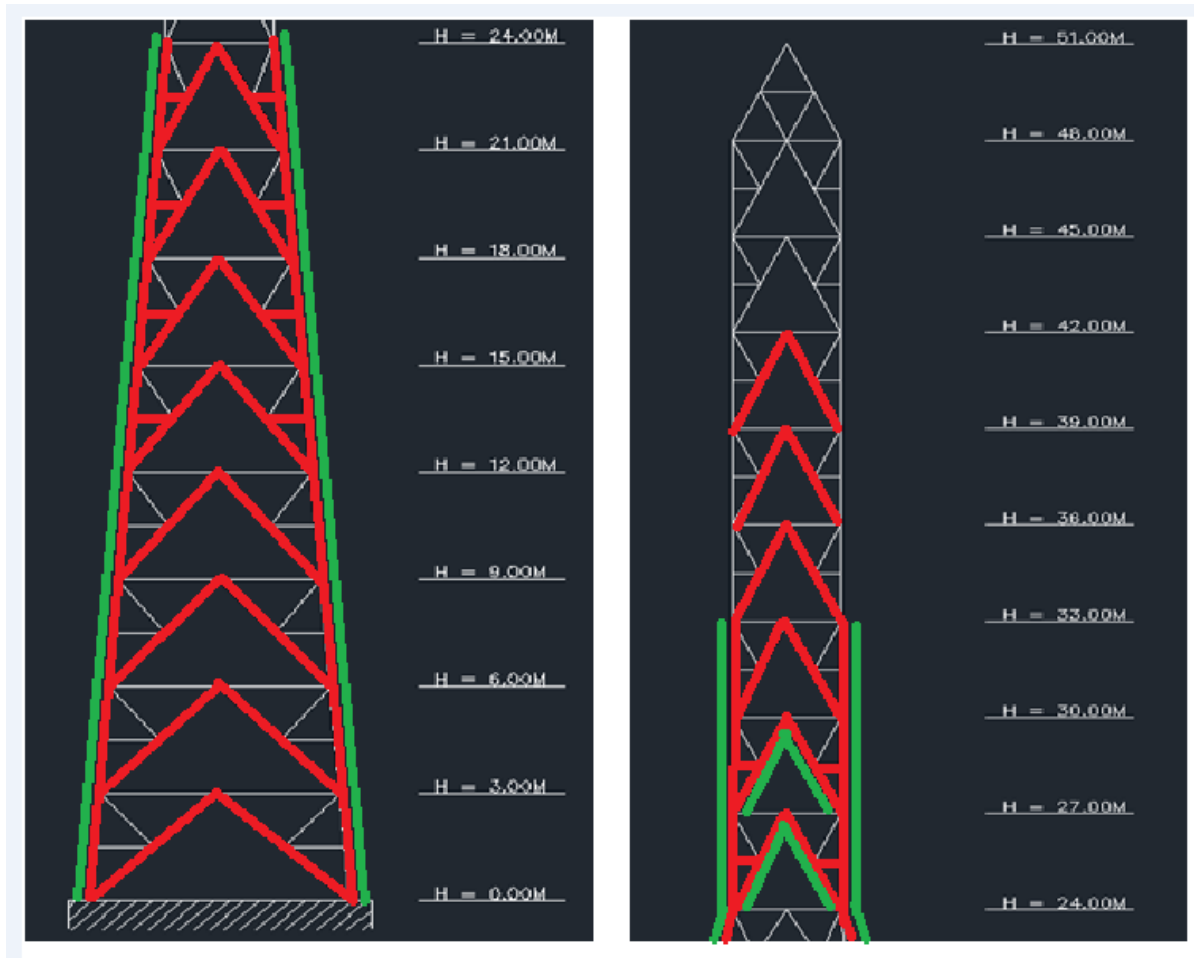
Figure 1.11: Designation of strengthened members

1.7.4 Results

Global analysis was followed by structural design, where all members are checked in accordance with EN 1993-1-1 and EN 1993-3-1 using the software package SOFISTIK-STEEL MEMBERS, against flexural buckling to compression and bending, lateral torsional buckling and buckling to pure compression.

In Table 1.8 the design results for each member type are given. The utilization factor for full exploitation of the cross-section is 1.00. Larger values indicate no permissible overloading of members.

Table 1.8: Maximum utilization factors for each member type of the strengthened tower

Tower members	Maximum utilization factor
Legs	1.03
Vertical diagonals	0.96
Horizontals	0.49
Secondary bracing members	0.93
Horizontal diagonal members	0.85
Members supporting climbing ladder	0.98

1.8 FRP strengthened tower

1.8.1 General

This paragraph concerns the design of a tower, same as the initial tower described in paragraph 1.6, strengthened using plates made from Carbon Fiber Reinforced Polymer (CFRP plates).

<u>Materials</u>

As it is mentioned in paragraph 1.3 the steel grade for all members of the tower is S235, with material safety factor 1.10.

For the strengthening of the tower Carbon Fiber Reinforced Polymer plates (CFRP plates) are used having various widths and thickness of 1.2 mm. Regarding the modelling, it is considered that the CFRP material is a linear material with properties as seen in Table 1.9.

Table 1.9: CFRP material's properties

Young's Modulus (E)	165 GPa	
Tensile strength	2900 MPa	
Compressive strength	210 MPa	
Ultimate strain	1.75 %	

<u>Cross sections</u>

Strengthening of the tower is implemented by application of CFRP plates made from the material described in Table 1.9. The CFRP plates are applied only to members that need to be strengthened according to the previous analysis of the initial tower, as described in paragraph 1.6. More specifically, the legs of the tower are strengthened up to the level of 33m, the vertical braces up to the level of 42m and the rest of the members are not strengthened, since it is not needed. The number of CFRP plates that are used varies along the height of the tower. At the tower's base and at heights from 24 to 30m strengthening is executed with more plates than at the other parts, because in these parts the largest axial forces develop. Figure 1.12 shows in a picture how the strengthening is executed along the height of the tower for legs and braces.

All the various (strengthened or not) cross sections that are used, together with their position along the height are shown in Table 1.10 (Legs) and Table 1.11 (braces). These tables show also the width of the CFRP plates used, which varies from 50mm to 150 mm, and how they are applied to angle sections. The other members of the tower are the same as the members of the initial tower and are shown in Table 1.3 (Initial Tower).
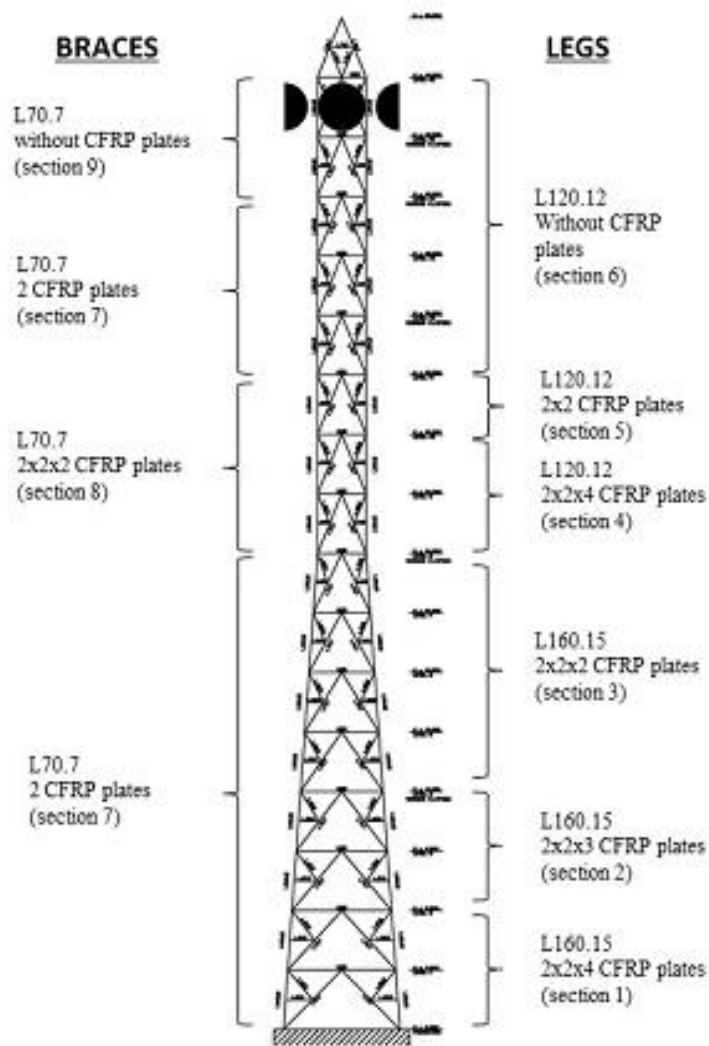
Figure 1.12: Tower strengthened with CFRP plates

Table 1.10: Leg's cross sections

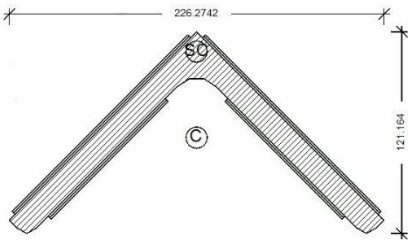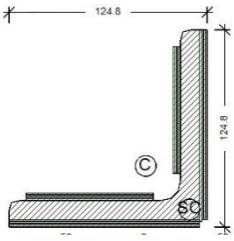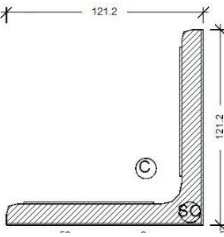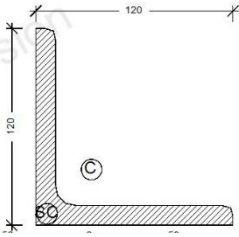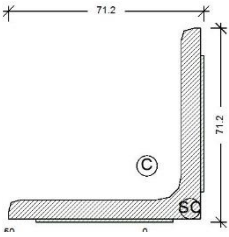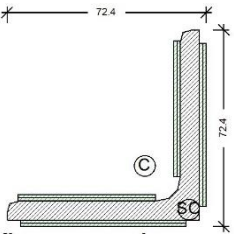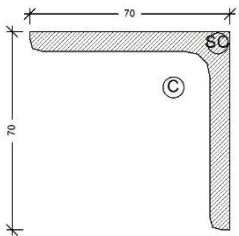| No	Legs:	Height	Section
1		0 – 6 m	L160.15 (initial) 2x4 CFRP plates S1512 (150x1.2 mm) 2x4 CFRP plates S1012 (100x1.2 mm)
2		6-12 m	L160.15 (initial) 2x3 CFRP plates S1512 (150x1.2 mm) 2x3 CFRP plates S1012 (100x1.2 mm)

3		12 - 24 m	L160.15 (initial) 2x2 CFRP plates S1512 (150x1.2 mm) 2x2 CFRP plates S1012 (100x1.2 mm)
4		24 – 30 m	L120.12 (initial) 2x4 CFRP plates S1212 (120x1.2 mm) 2x4 CFRP plates S812 (80x1.2 mm)
5		30 – 33 m	L120.12 (initial) 2x1 CFRP plates S1212 (120x1.2 mm) 2x1 CFRP plates S812 (80x1.2 mm)
6		33 – 48 m	L120.12 (initial) Without CFRP plates

Table 1.11: Brace's cross sections

No	**Braces:**	Height	Section
7		0 – 24 m and 33 – 42 m	L70.7 (initial) 2x1 CFRP plates S512 (50x1.2 mm)
8		24 – 33 m	L70.7 (initial) 2x2 CFRP plates S612 (60x1.2 mm) 2x2 CFRP plates S512 (50x1.2 mm)
9		42 - 48 m	L70.7 (initial) Without CFRP plates

1.8.2 Design loads

The CFRP plates are applied on the existing legs and bracings, so the reference area that is considered for the calculation of the Wind loads is equal to that of the initial tower. Actually, there is a small increase (less than 4%) which can be ignored. The self-weight of the CFRP plates can also be ignored, since it is small (less than 0.5% of the total weight of the tower).

Based on the above, it is assumed that the design loads and the load combinations of the strengthened tower are the same as the loads acting on the initial tower, which are calculated and presented in paragraph 1.4, 1.5 and 1.7.2.

1.8.3 Global analysis and design

The strengthened tower was modelled and analysed using the SOFISTIK finite element software. The strengthened members are simulated as by means of 6DOF beam elements with a new composite section, that consists of the steel section and the CFRP plates. The new composite sections of the strengthened members (legs and braces) were designed using the section designer tool of the software as shown in Table 1.10 and Table 1.11.

Some major design assumptions are summarized below:

- Hinges are assigned to the ends of all braces and horizontal members.
- There is no eccentricity in beam's connections, all members are simulated as centric beam elements.
- The foundations for the legs are modelled as pinned supports.

Characteristic pictures of the numerical model are shown in Figure 1.13.
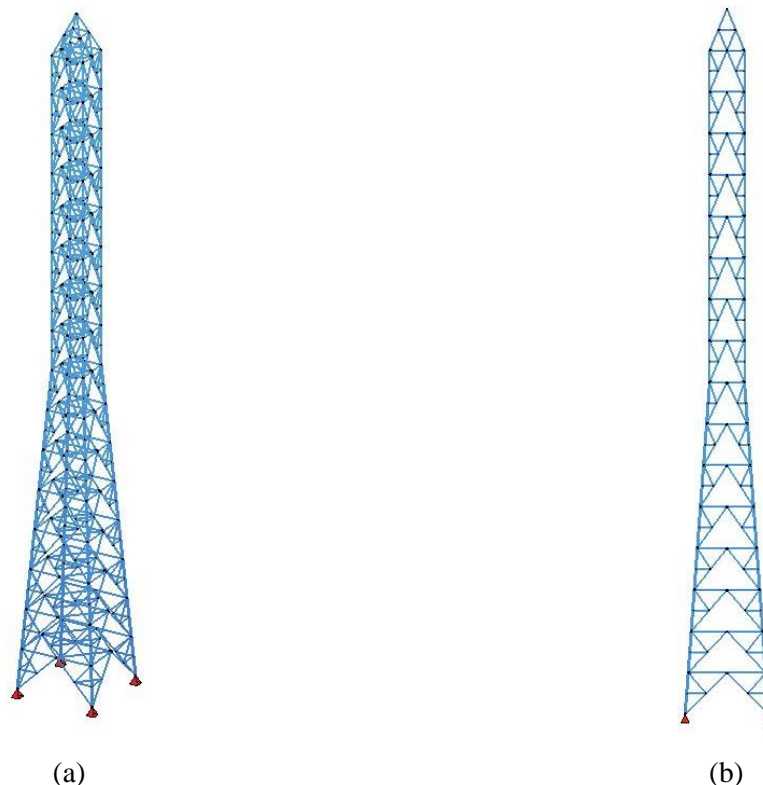

(a) (b)

Figure 1.13: Three-dimensional structural model used for the analysis of the tower: a) prospective view b) side view

At first, Modal Analysis was performed to determine the natural frequencies of the tower. The first modes and the corresponding periods are shown in Figure 1.14. Due to structure's and loads' symmetry the first two modes have the same period but refer to different (major) direction. The 3rd mode is torsional.
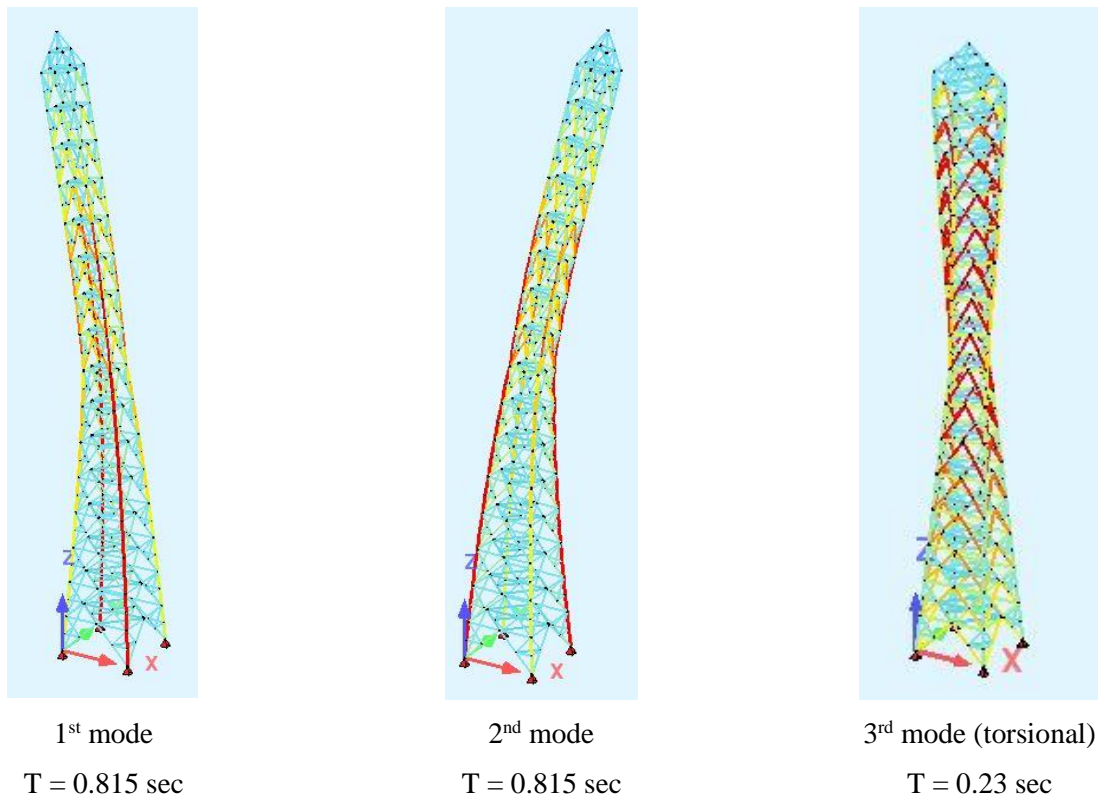
1st mode	2nd mode	3rd mode (torsional)
T = 0.815 sec	T = 0.815 sec	T = 0.23 sec

Figure 1.14: First Modes

Then, 3rd order analysis was performed to verify the stability of the structure, the plasticity level and the utilization factor of each members. In 3rd order analysis, both nonlinear material and geometrical nonlinearity is taken into account. This type of analysis was used instead of linear analysis, because it is quite complicated to calculate the buckling resistance and make the relevant verifications of the strengthened members, with the new composite section (CFRP plate and angle section), in accordance with Eurocodes.

Figure 1.15 shows the deformed shape of the tower, enlarged by 10 for better display, as well as the horizontal displacement at each level. The maximum displacement at the top of the tower is 397 mm, which corresponds to a vertical angle of the parabolic antennas equal to 0.57 degrees.
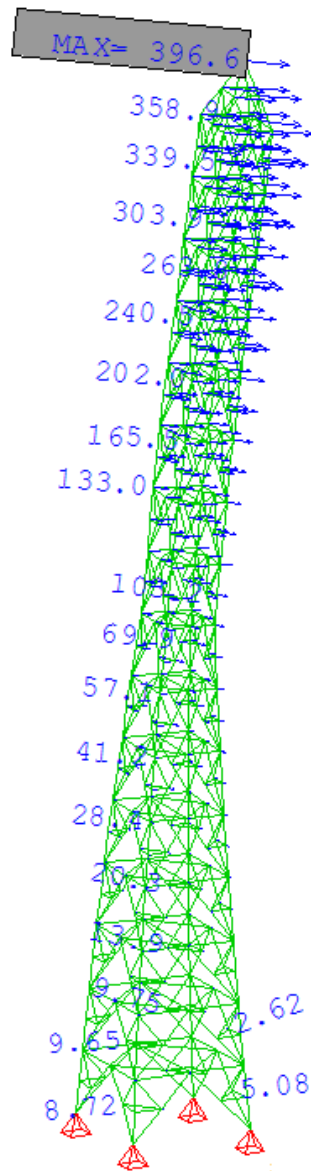
Figure 1.15: Tower's deformed shape and horizontal displacements at each level

The results of the analysis are summarized below.

The maximum total utilization factor of each group of members is shown in Table 1.12.

Table 1.12: Maximum utilisation factor for members

Group of members	Maximum utilisation factor
Legs	0.991
Vertical Braces	0.967
Horizontal members	0.431
Secondary and horizontal braces	0.606
horizontal members	0.158
Horizontal braces at platform's level	0.445
Members at the top of the tower	0.063

The utilisation factor of the legs and braces along the height of the tower is shown in Figure 1.16.

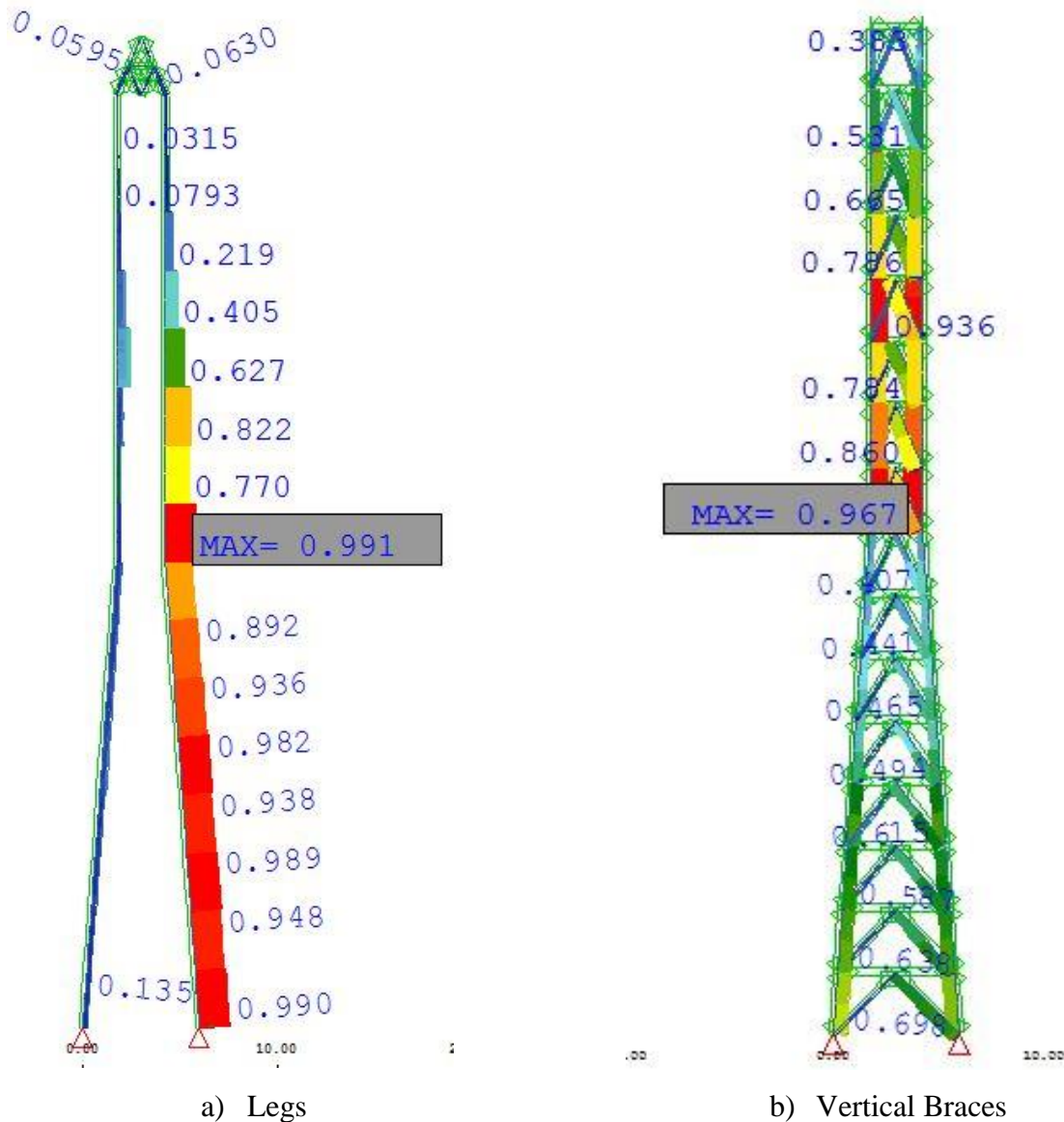a) Legs   b) Vertical Braces

Figure 1.16: Utilisation factor along the height of the tower for a) Legs and b) Braces

The maximum stresses that develop in the Leg and Brace sections are shown in Table 1.13 and Table 1.14. It is noticed that for the most unfavourable load combination the steel section yields, while the CFRP plates almost reach their compressive strength, which was considered as only 6% of the tensile strength.

Table 1.13: Maximum stresses on steel (material 1)

Mat	Check or Criterion		Value	Limit	Unit	Level
1	Centric compression	σ-n,c	187.11	213.64	MPa	0.876
	Centric tension	σ-n,t	164.92	213.64	MPa	0.772
	Longitud. compressive stress	σ-x	249.02	213.64	MPa	**1.166**
	Longitud. tensile stress	σ+x	220.49	213.64	MPa	**1.032**
	Shear stress	τ	18.59	123.34	MPa	0.151
	Von Mises stress	σ-v	249.02	213.64	MPa	**1.166**
	Shear in weldings			207.85	MPa	
	Compression in compr. zone	σc-0	187.11	213.64	MPa	0.876
	Plate slenderness c/t			1.00		

Table 1.14: Maximum stresses on CFRP (material 3)

Mat	Check or Criterion		Value	Limit	Unit	Level
3	Centric compression	σ-n,c	147.01	210.00	MPa	0.700
	Centric tension	σ-n,t	129.38	2900.00	MPa	0.045
	Longitud. compressive stress	σ-x	193.97	210.00	MPa	0.924
	Longitud. tensile stress	σ+x	171.78	2900.00	MPa	0.059
	Shear stress	τ	18.00	1674.32	MPa	0.011
	Von Mises stress	σ-v	193.97	2900.00	MPa	0.067
	Shear in weldings			1488.28	MPa	
	Compression in compr. zone	σc-0	147.01	210.00	MPa	0.700
	Plate slenderness c/t			1.00		

Further on Modal Response spectrum analysis was performed to verify the member's capacity for the Earthquake load combination defined in paragraph 1.5. The base shear on both directions for this combination was calculated using the CQC method and is shown in Table 1.15.

Comparing the base shear for the Earthquake combination with the total lateral force that occurs for the most unfavorable wind load combinations (Table 1.16 and Table 1.17), it is noticed that it is quite smaller, so further members' verifications are omitted.

Table 1.15: Base shear for the Earthquake combination

Sum of forces (Base-Shear)

LC	H	Mode	Vb		
	[m]		X[kN]	Y[kN]	Z[kN]
990	base[1]	CQC[2]	133.0	3.1	0.0
991	base[1]	CQC[2]	3.1	132.8	0.0

Table 1.16: Total lateral force for the most unfavourable load combination (diagonal wind)

Sum of Loadings

Loadcase	Σ(Loads)		
	X[kN]	Y[kN]	Z[kN]
1016	255.2	255.2	-289.3

Table 1.17: Total lateral force for the most unfavourable load combination (orthogonal wind)

Sum of Loadings

Loadcase	Σ(Loads)		
	X[kN]	Y[kN]	Z[kN]
1015	0.0	302.0	-289.3

1.8.4 Conclusions

This chapter addressed the design of a typical telecommunication tower strengthened with CFRP plates. Strengthening towers by using CFRP plates proved to be a possible solution, which has certain advantages comparing with the conventional strengthening method. The main advantage is that using CFRP plates there is no increase in the wind loads, since CFRP plates apply on existing members. On the other conventional strengthening method uses star battened configuration for legs and larger profiles for braces, which results in the increase of the wind loading and the self-weight of the structures.

In addition, this method of strengthening needs less time to be accomplished, less equipment and construction machinery. Therefore, it can be applied easily on mountainy and inaccessible areas in short time.

The total length of the CFRP plates that are needed is calculated and is shown in Table 1.18. The thickness of all plates is 1.2mm. Based on this, several parameters of the strengthening procedure can be estimated, such as the total cost and the total time of construction.

Table 1.18: Total length of CFRP plates

CFRP code	Width (mm)	Total Length (m)
S1512	150	132
S1212	120	54
S1012	100	132
S812	80	54
S612	60	36
S512	50	102

2 Transmission towers

2.1 Introduction

In Europe, the design of transmission towers for overhead electrical lines can be carried out according to EN 1993-3-1: 2006 [1] or for electrical lines exceeding 1 kV according to EN 50341-1: 2012 [2]. Both standards prescribe linear elastic global analyses for the design of steel lattice towers, adopting some common assumptions for the modelling. Then the members and sections are checked by means of specific design rules. The TOWER [3] software is aimed at implementing automatically this approach and will be used to reach the first main objective of this study: to design a typical transmission tower according to the existing norms and especially based on EN 50341-1: 2012 [2].

Then, the second main objective is to validate the design which will be initially done with TOWER software. For this purpose, the tower will be simulated with the FINELG [4] non-linear finite element software. The comparison between both software will be achieved at two levels: results of the frame analysis in the elastic range and then at factored design loads.

But to have a global overview of the actual tower's response, an elastic instability analysis will be performed and will be complemented by a second order linear elastic one. Then a non-linear plastic analysis will be achieved so as to evaluate the influence of plasticity on the tower response. Finally, the influence of the initial imperfections will also be investigated.

However, material and geometrical non-linearities combined with imperfections (out-of-straightness of a member, out-of-plane) will affect the response of the tower. Therefore, at the end, as a third main objective of this study, a full non-linear analysis will be performed by FINELG to check the validity of the initial design made with the TOWER software. Furthermore, the non-linear (push over) analysis give the possibility to explore the potential inelastic redistributions in the tower.

2.2 Design specifications

A stated in the report "Structural typologies for telecommunication and transmission towers", the Danube tower is the most spread tower typology for transmission lines in Europe. In addition, many transmission lines are currently in planning throughout Europe in the framework of the conversion from 220 kV to 380 kV lines, where the Danube tower is the favourite typology of the designers and owners. As a result, the Danube tower (Figure 2.1) is the typical typology of current and future transmission lines and is therefore selected for the case studies presented in this chapter.

Figure 2.1: Danube tower for a transmission line of 380 kV

2.2.1 Geometry of the tower

The case study involves a standard Danube tower with a standard height of 50 m (Type D 16). The annotations of the different segments of the tower are indicated in Figure 2.2.
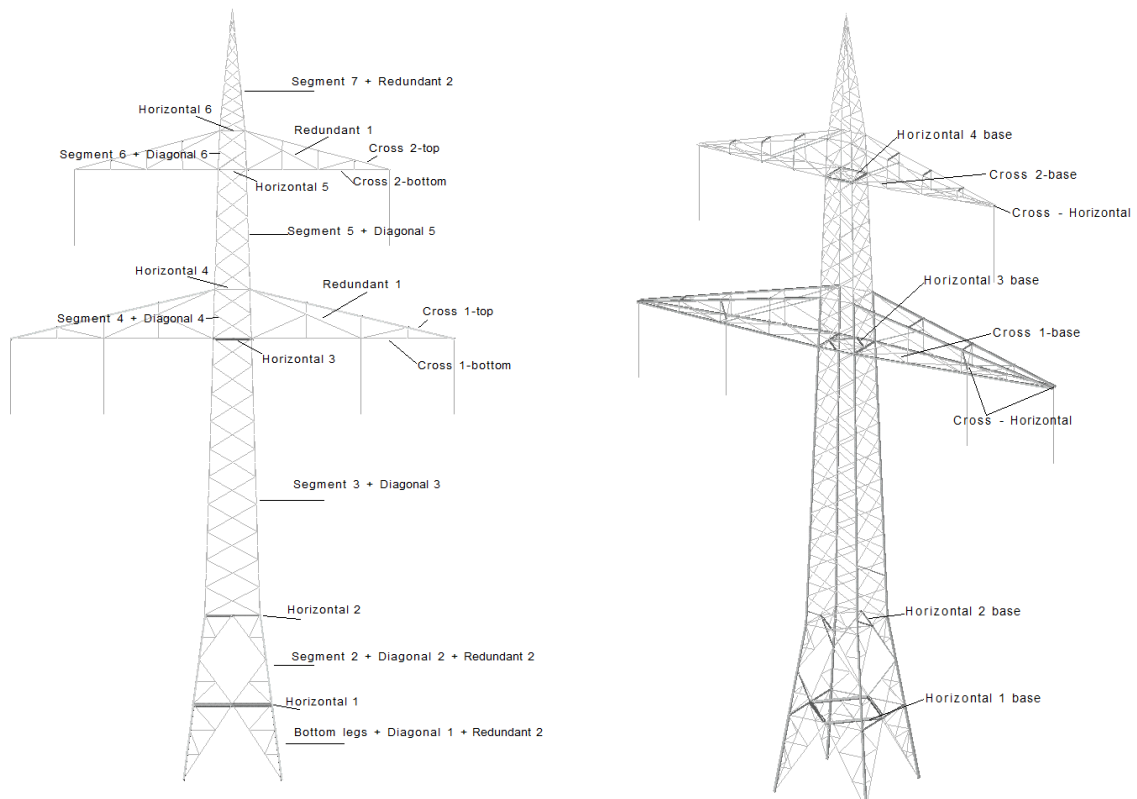

Figure 2.2: Annotations of the different segments of the tower

The geometry and the dimensions of the tower are indicated in Figure 2.3 to Figure 2.9. The tower is a suspension tower (i.e. hanging insulators) made of hot-dip galvanized equal-leg angle profiles.
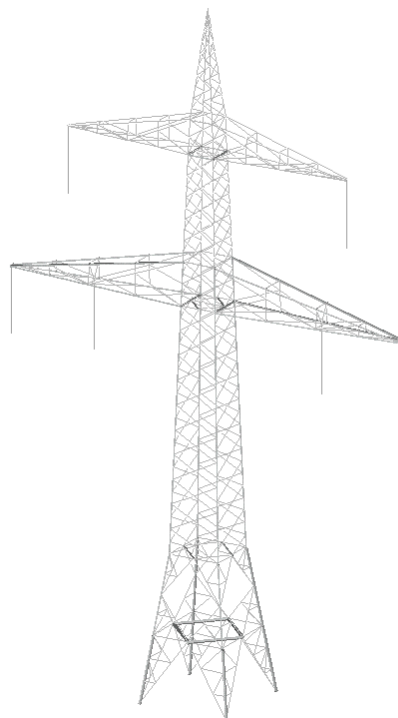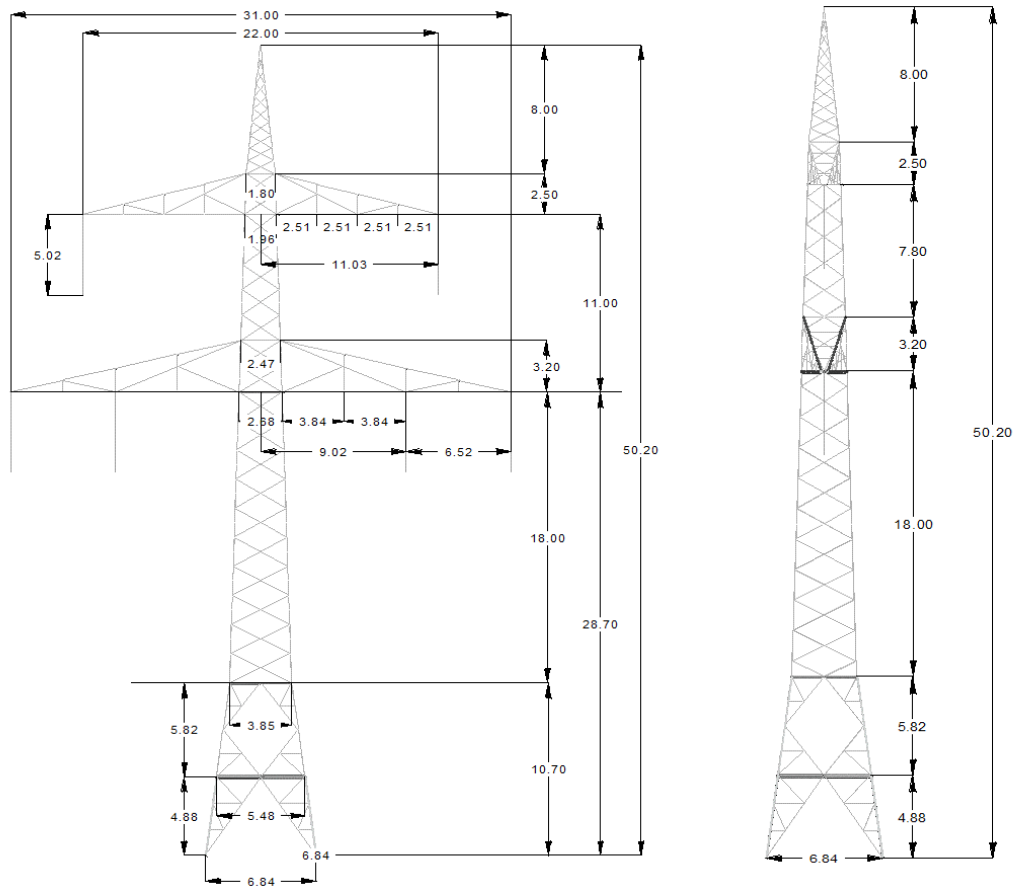

Figure 2.3: Isometric view of the Danube tower
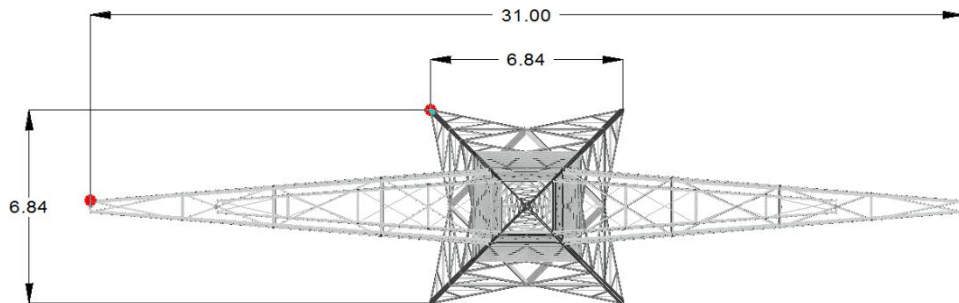
Figure 2.4: Dimensions of the Danube tower

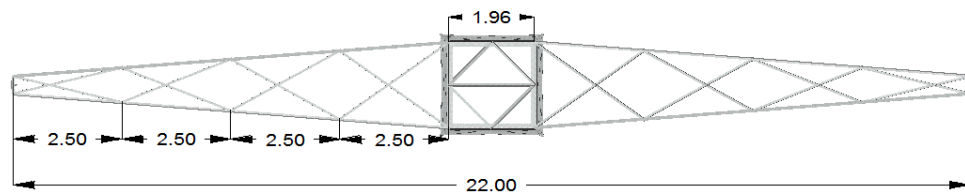**Figure 2.5: Top view of Danube tower**

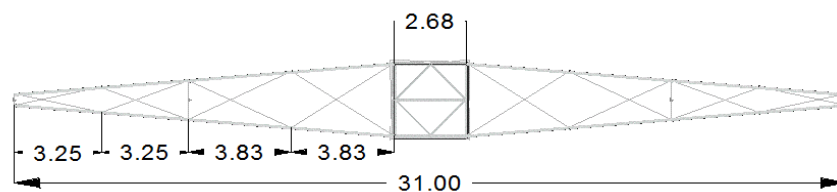**Figure 2.6: Base of lower cross arm**

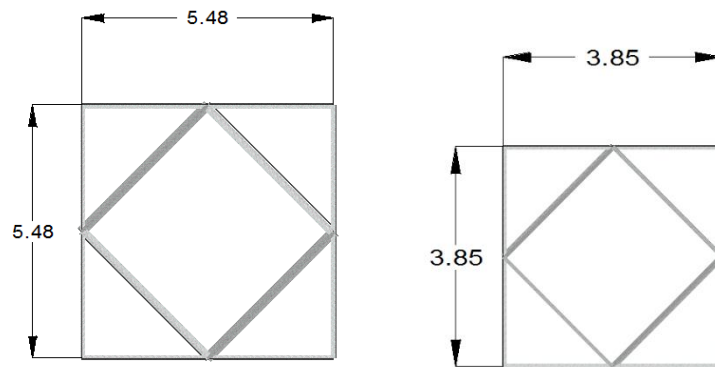**Figure 2.7: Base of top cross arm**

Figure 2.8: Horizontal bracings: Horizontal 1 (left) and Horizontal 2 (right
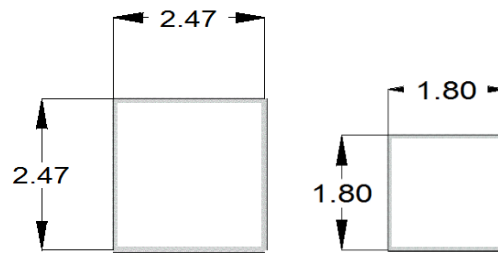
Figure 2.9: Horizontal bracings: Horizontal 4 (left) and Horizontal 6 (right

The foundation consists in four step foundations, one for each leg profile. Secondary bracings (i.e. redundant members) additionally decrease the buckling length of the primary bracing members and legs in Segment 1 and Segment 2 (Figure 2.4). The buckling length of the leg profiles is reduced by a staggered vertical bracing configuration for Segment 3 to Segment 5 and Segment 7 (Figure 2.10).
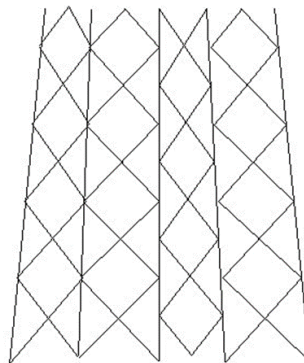
Figure 2.10: Staggered bracing

2.2.2 Conductors and insulators

The tower carries two 380 kV circuits, which each consists of 3 phases. Each phase is made of a bundle of 4 conductors which is supported by a suspension insulator. On its top, the tower carries one single earth wire for lightening protection. The conductors and the earth fire are made of steel fibres enveloped by several fibres of aluminium (Figure 2.11). The steel fibres reinforce the conductors and allow a safe transfer of the conductor loads while the aluminium fibres increase the conductivity of the conductor.

The following conductors according to EN 50182:2001 [5] are selected for the Danube tower of the case study:

- 4*264-AL1/34-ST1A for the conductors;
- 1*94-AL1/15-ST1A for the earth wire.

The notations of the conductors according to [5] are explained below:

The first numerical factor "4" stands for the four bundles forming each conductor. The designation "264-AL1" identifies a surface area of the aluminium fibres of 264 mm² and in a similar way, the designation "34-ST1A" describes a surface of 34 mm² of the steel fibres. Important mechanical data of the conductors and the earth wire can be taken from Table 2.1.

Figure 2.11: Aluminium-steel conductor

Table 2.1: Mechanical data for the conductors

Code	Areas			No. of wires		Wire diameter		Mass per unit	Final modulus	Coefficient of linear
	Al	Steel	Total	Al	Steel	Al	Steel			
	mm²	mm²	mm²	mm²	mm²	mm²	mm²	kg/km	N/mm²	1/K
94-AL1/15-ST1A	94,4	15,3	109,7	26	7	2,15	1,67	380,6	77 000	1,89E-05
264-AL1/34-ST1A	263,7	34,1	297,7	24	7	3,74	2,49	994,4	74 000	1,96E-05

Each conductor is connected to a suspension insulator, which transfers the conductor loads to the cross arms of the lattice tower. The insulator (Figure 2.12) is made of silicone rubber (Quadri*Sil Insulator from the company Hubbell) with increased life-time and a reduced self-weight compared to glass insulators.

Figure 2.12: Quadri*Sil insulator S025185S201

The length of the insulator is about 5 m to ensure a safe distance between the conductors of the 380-kV line and the tower structure. The weight of one insulator is about 9 kg (≈ 87 N).

2.2.3 Material

All members of the tower are made of steel grade S355J2. Bolts and gusset plates are possibly made of different steel grades than the whole tower. However, at the level of a global analysis, as addressed in this chapter, they are not simulated. Two cases are considered bellow in terms of

material law: a linear elastic one and a non-linear full plastic one. The parameters for each case are defined bellow.

2.2.3.1 Linear elastic material law

The steel material law is linear elastic without any yielding plateau. The properties used for the structural analysis and design are shown in Table 2.2. For the analyses, the safety factors for the material resistance are assumed equal to 1,0. Nevertheless, this does not affect at all the results for the linear elastic (1st or 2nd order) and instability analyses. For the design checks through TOWER, values different than 1,0, are adopted (see 2.3.1).

Table 2.2: Material's properties

Material	S355J2	linear elastic law	
Young's modulus	E	210000	[N/mm^2]
Poisson coefficient	v	0,3	[-]
Shear modulus	G	80770	[N/mm^2]
Density	ρ	7850,0	[kg/m^3]
Weight	γ	78,5	[kN/m^3]

2.2.3.2 Non-linear plastic material law

The steel material law is elastic-perfect plastic. The properties used for the structural analysis are shown in Table 2.3 and Figure 2.13. The safety factors for the material resistance are equal to 1,0.

Table 2.3: Material's properties

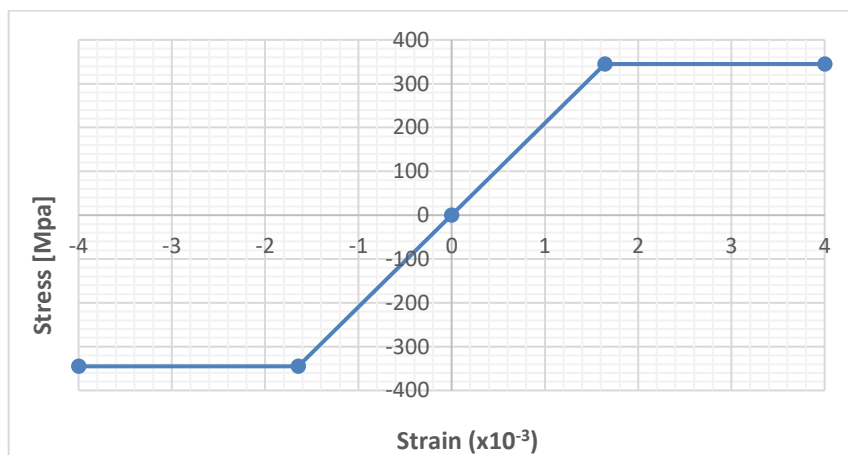| Material	S355J2	Full plastic law	
Young's modulus	E	210000	[N/mm^2]
Poisson coefficient	v	0,3	[-]
Shear modulus	G	80770	[N/mm^2]
Density	ρ	7850,0	[kg/m^3]
Weight	γ	78,5	[kN/m^3]
Yield stress	fy	345	[N/mm^2]

Figure 2.13: Stain – Stress curve

In addition, for each element, residual stresses which result from hot-rolling procedure are considered; the pattern is shown in Figure 2.14. This pattern, found in many scientific papers [6], is also been used as a reference for the development of Eurocode 3 design rules.
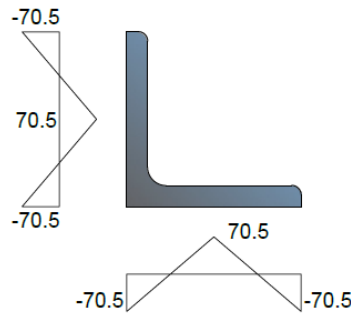
Figure 2.14: Residual stresses of angle cross-section

2.2.4 The transmission line

In the framework of the present case study, only the lattice steel tower is designed. The overall transmission line is not investigated in the present project. The design of the tower structure however requires some basic information of the transmission line in order to quantify the conductor loads acting on the tower.

It is supposed that the Danube tower is part of a 380-kV transmission line with a distance between the towers of 350 m. Furthermore, the line is supposed to be straight along the segment the tower is part of. The segment of the line is in a mountain area (see section 2.2.5) with significant height differences, which leads to the following spans of the line (Figure 2.15):

- Wind span: $s_w = 350$ m
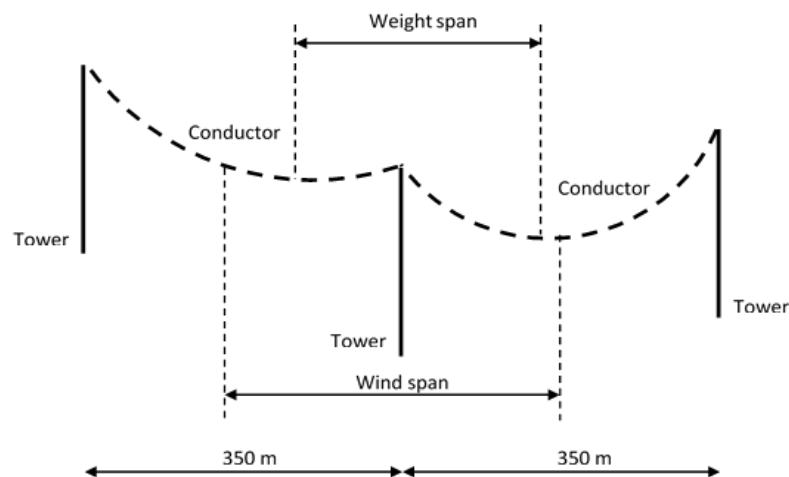- Weight span: $s_g = 1,5 \cdot 350$ m $= 525$ m (according to [7])

Figure 2.15: Definition of wind span and weight span

The wind span is equal to the mean value of the two neighbouring spans of the tower while the weight span is equal to the distance between the two lowest points of the conductors in the two neighbouring spans of the tower.

2.2.5 Location of the tower

The transmission line is supposed to be in the "Erzgebirge" in Saxony, Germany. According to EN 50341-2-4:2016 [8], the German national annex of EN 50341-1:2012, the region is located in wind zone 2 (Figure 2.16). Since it is a mountain region with a high amount of ice to be expected, ice load zone E2 according to [8] is applied for the determination of the ice loads on the conductors and the insulators.

Figure 2.16: Location of the transmission line: Erzgebirge in Saxony, Germany

2.3   Design of the tower – Linear elastic global analyse with TOWER

2.3.1   General design assumptions

The linear elastic global analyse of the tower is carried out according to [8].

The major design assumptions of the German national annex are summarised below:

- The internal forces are determined using elastic global analyses and first order theory.
- Lattice steel towers are considered as pin jointed truss structures.
- The safety factors for the material resistance for the design checks are $\gamma_{M0} = 1,1$; $\gamma_{M1} = 1,1$ and $\gamma_{M2} = 1,25$.
- 12 different load cases (from load case A to load case L) are to be considered (see paragraph 2.3.2)
- Ice loads on the tower structure are not considered.
- The stipulated wind loads are based on DIN EN 1991-1-4/NA:2010-12 [9]. The German National annex applies method 1 of [2]: the tower is subdivided into several segments and the wind force acts in the centre of gravity of each section.
- The stipulations for ice loads are based on a study of the German Meteorological Services (DWD) and long-term operational experience (Ice load zones).
- The eccentricities of the connections are considered via an effective non-dimensional slenderness λ_{eff}.
- The German national annexe allows the buckling verification of the angle profiles using buckling curve c as defined in [1].
- The out-of-plane buckling verification of the crossing diagonals is based on the ratio between the force in the supporting member and the force in the compression member.

The bolted connections between the different diagonal and leg members as well as the splices of the legs are not considered in the design. The foundations are assumed as pin supports.

2.3.2   Load cases

As stated in paragraph 2.3.1, the German National annex of [2] defines 12 different standard load cases. The load cases cover meteorologically caused forces (i.e. wind and ice), construction and maintenance loads and exceptional loads due to unbalanced ice loads or conductor rupture.

Each load case combines loads of different origin, which are assumed to act simultaneously. The design value of actions is given in [8] as follows:

$$E_d = \{\gamma_G G_K; \ \gamma_w Q_{WK}; \ \gamma_I Q_{IK}; \ \gamma_P Q_{PK}; \ \gamma_C Q_{CK}\}$$

where:

E_d total load;

G_K dead load of conductors, insulators and supports;

Q_{WK} wind forces as specified in 4.4.1/DE.1 in [8];

Q_{IK} ice loads on conductors as specified in 4.5.2/DE.1 [8];

Q_{PK} construction loads in 4.9.1/DE.1 and 4.9.2/DE.1;

Q_{CK} horizontal conductor tensile forces considering the temperature changes as well as wind and ice loads as specified in 4.12.2/DE.1 in [8].

In detail, the following standard load case according to [8] are considered in the design of the tower:

Load case A:
Permanent loads, wind forces in direction of the cross arms (x-direction in Figure 2.17).

Load case B:
Permanent loads, wind forces transversal to the cross arm (y-direction in Figure 2.17).

Load case C:
Permanent loads, wind forces at $\phi = 45°C$.

Load case D:
Permanent loads, wind forces in direction of the cross arms and ice loads.

Load case E:
Permanent loads, wind forces transversal to the cross arms and ice loads.

Load case F:
Permanent loads, wind forces at $\phi = 45°C$ and ice loads.

Load case G:
Permanent loads and ice loads in one of the adjacent spans, no ice loads in the other adjacent span, whereby 50% of the ice loads is assumed.

Load case I:
Permanent loads and construction loads. The construction loads consist in vertically acting point load of 1 kN to be positioned at the most unfavourable node of the cross arms

Load case J:
Permanent loads and ice loads.

The partial safety factors to be applied to the loads depend on the load case and are as follows [8]:

- $\gamma_G = \gamma_W = \gamma_I = \gamma_P = \gamma_C = 1{,}35$ for load cases A to I in case of unfavourable action;
- $\gamma_G = \gamma_I = 1{,}35$ for load cases A to F in case of favourable action
- $\gamma_G = \gamma_W = \gamma_I = \gamma_P = \gamma_C = 1{,}0$ for load cases J to L (exceptional load cases)
- $\gamma_P = 1{,}5$ for construction loads in load case I

The tension loads in the conductors at different temperatures and the load cases H, K and L are not considered in the design of the tower since it is a suspension tower.
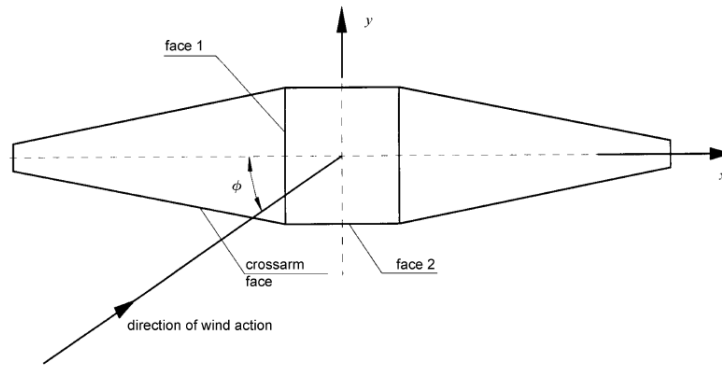
Figure 2.17: Definition of wind direction

In addition to the standard load cases, the load case "weight of lines men" shall be considered: for members with an angle to the horizontal less than 30°, a point load of 1 kN acting in the centre of the member must be assumed. No other loads need to be considered for this load case.

2.3.3 Design checks

The steel lattice tower of the present case study is designed according to [8]. The following verifications are carried out:

- Section verifications

The section verifications comprise the tension resistance checks of the angle profiles. The verifications are carried out according to J.3, Annex J of [8].

- Member verifications

The member verifications consist in the buckling verifications of the angle profiles. Flexural, torsional and torsional flexural buckling are verified according to J.4, Annex J of [8]. The cross section is classified according to Table 5.1 in EN 1993-1-1:2005 [10] and for cross section class 4, the effective cross section area A_{eff} is determined according to 7.3.6.2 in [2].

- Verification of inclination of bracings

According to 7.3.5/DE.2 in [8], the inclination of the bracings to the horizontal may not be more than 45°.

- Redundant member verification

The redundant members (secondary bracings) are verified according to J.4.4 in [8]. For the design of the redundant members, a hypothetical force of 2 % of the force in the main member is applied transversally to each node of the redundant members.

2.3.4 Design in software TOWER

The design of the steel lattice tower is carried out in software TOWER – Version 15.0. TOWER is a software which is dedicated to the design of transmission and communication steel lattice towers. The software is based on generic finite element programme SAPS [3]. Three element types are used in TOWER: truss, beam and cable elements.

TOWER offers the possibility to design steel lattice towers according to different international standards (e.g. ASCE 10-97, EN 50341-1:2012, BS-8100). In addition, it allows the design according to different National Annexes of EN 50341-1:2012. Although [8] is not covered by TOWER, it is possible to carry out a design according to its prescriptions by manually adapting some factors. This procedure has been followed for the design of the tower in the present case study.

Moreover, TOWER also supports nonlinear analyses of steel lattice towers. In a nonlinear analysis, the material is still supposed to be linear and TOWER solely accounts for geometric nonlinearities.

A major advantage of TOWER consists in its automatic optimization processes. The full optimization algorithm automatically adapts the size, the type and the steel grade (if required by the user) of the angle profiles to finally propose the lightest structure with at the same time the highest utilization degree. Hereby TOWER assumes that the weight of the structure is proportional to its costs. The user has the possibility to select the range of angle sizes and types within those the optimization algorithm should select the best solutions.

The tower structure in the present case study (see paragraph 2.2.1) is modelled using the following elements:

- leg members are modelled with beam elements (in green in Figure 2.18);
- primary bracings are modelled with truss elements (in blue in Figure 2.18);
- secondary bracings (redundant members) are modelled with truss elements (in orange in Figure 2.18).

In this way, the occurrence of planar joints (joints with no stiffness perpendicular to elements plane) is avoided.
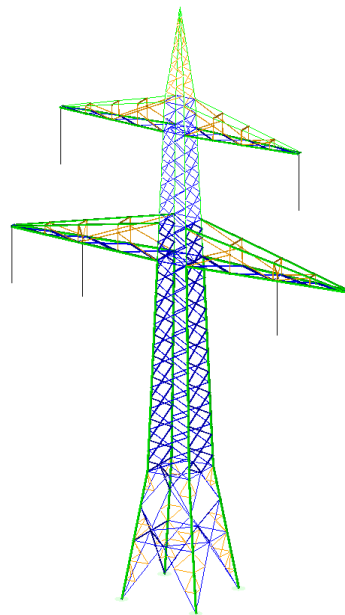

Figure 2.18: Model of the Danube tower in the software TOWER

Bolts and gusset plates are not modelled in TOWER (i.e. pin jointed truss structure). Their self-weight is accounted for by a so called "Dead load adjustment factor" which is entered by the user. The factor artificially increases the dead loads of the tower to consider the weight of the bolts and the gusset plates. For the present case study, a factor of 1,2 is applied (e.g. the self-weight of the modelled structure is amplified by 20 %).

The steel grade for the angle profiles is fixed to S355J2. In TOWER, the steel material law is linear elastic without any plastic yield plateau (see paragraph 2.2.3.1). The material parameters in TOWER are slightly more conservative than the values in [10] but they are safe-sided.

The conductors cannot be modelled in TOWER. The wind and ice loads on the conductors and the earth wire as well as their self-weight are calculated apart (i.e. by hand and according to [8]) for each load case (see section 2.3.2) and entered in TOWER as point loads acting on the tip of the insulators. Tension loads in the conductors are not considered since it is a suspension tower.

Following [8], ice loads on the tower body are not considered in the design. The foundations for the legs are modelled as pinned supports.

The linear elastic global design is carried out in TOWER considering the prescriptions of [8] and using the full optimization option of the design software. The results are presented in section 2.3.5.

2.3.5 Results of the linear elastic global design

The results of the linear elastic global analyses finalized with TOWER according to [8] are presented in Table 2.4. For the annotations of the different segments of the tower, see Figure 2.2.

Table 2.4: Angle profiles for the different sections of the tower

Group	Angle Type	Angle Size	Steel grade
Bottom-legs	SAE	AM 150x150x13-/+	S355J2
Segment 2	SAE	AM 140x140x15	S355J2
Segment 3	SAE	AM 120x120x16	S355J2
Segment 4	SAE	AM 80x80x10-	S355J2
Segment 5	SAE	AM 80x80x6	S355J2
Segment 6	SAE	AM 75x75x4	S355J2
Segment 7	SAE	AM 45x45x3	S355J2
Diagonal 1	SAE	AM 75x75x4	S355J2
Diagonal 2	SAE	AM 75x75x4	S355J2
Diagonal 3	SAE	AM 90x90x5	S355J2
Diagonal 4	SAE	AM 90x90x6	S355J2
Diagonal 5	SAE	AM 60x60x4	S355J2
Diagonal 6	SAE	AM 45x45x4	S355J2
Cross 1-bottom	SAE	AM 150x150x12-/+	S355J2
Cross 1-top	SAE	AM 120x120x7	S355J2
Cross 1-base	SAE	AM 130x130x8	S355J2
Horizontal 1	SAE	AM 80x80x5	S355J2
Horizontal 2	SAE	AM 90x90x5	S355J2
Horizontal 3	SAE	AM 100x100x7	S355J2
Horizontal 4	SAE	AM 76x76x4.8	S355J2
Horizontal 5	SAE	AM 75x75x6-	S355J2
Horizontal 6	SAE	AM 65x65x4	S355J2
Horizontal 1 base	SAE	AM 80x80x5	S355J2
Horizontal 2 base	SAE	AM 80x80x5	S355J2
Horizontal 3 base	SAE	AM 76x76x4.8	S355J2
Horizontal 4 base	SAE	AM 60x60x4	S355J2
Cross - Horizontal	SAE	AM 45x45x3	S355J2
Cross 2-bottom	SAE	AM 120x120x7	S355J2
Cross 2-top	SAE	AM 75x75x5	S355J2
Cross 2-base	SAE	AM 90x90x5	S355J2
Redundant 1	SAE	AM 90x90x5	S355J2
Redundant 2	SAE	AM 60x60x4	S355J2
Redundant 3	SAE	AM 90x90x5	S355J3

*SAE: Equal leg angels

The total weight of the structure is 16,996 tons. The total weight includes the weight of the angle profiles, the weight of the insulators and the weight of the bolts and gussets which is estimated by the dead load adjustment factor of 1,2.

The results coming from the linear elastic global analyses of the Danube tower are compared to the results obtained from a first order linear elastic analysis and a full nonlinear analysis of the same tower through FINELG software.

2.4 Loads, load combinations and types of analyses with FINELG

The loads and the load combinations that will be used in the analysis performed by FINELG, are summarized in this paragraph as well as the different types of analyses that are to be performed.

2.4.1 Applying loads

The loads that are applying to the tower, including the loads from the conductors, are summarized below. Ice loads are not considered.

A.1 Self-weight of tower

The self-weight of the tower itself, is calculated automatically from the analysis program according to the geometry, considering the specific weight of steel γ=78,5 kN/m³.

Bolts and gusset plates are not modelled also with FINELG, but their self-weight taken into account by an adjustment factor equal to 1,20 which artificially increases the dead loads of the tower. This leads to a total weight of the tower of 172,60 kN.

A.2 Self-weight of conductors and earth wire

The self-weight calculations of the conductors (the value is given for one conductor) and the earth wire cable, are evaluated according to EN 50182 [5] and summarized in Table 2.5.

Table 2.5: Self-weight of conductors and earth wire

Type / Code	Mass per unit length [kg/km]	Weight span L_g [m]	g_c [N/m]	Bundles	$V_{c,i}$ [kN]
1 Conductor 264-AL1/34-ST1A	994,4	525	9,755	4	20,486
Earth wire 94-AL1/15-ST1A	380,6	525	3,734	1	1,960

A.3 Self-weight of insulators

The weight of one insulator is about 0,087 kN. Consequently, for the six insulators which have been used, the total weight equals 0,522 kN.

B.1 Wind loads at the tower

The calculation of the wind loads on the tower is based on EN 1993-3-1/Annex B/B.3.2.2.1 and EN 1991-1-4. The tower is subdivided into several segments and for each segment a mean wind load is evaluated. The mean wind load in the direction of the wind on the tower for a segment, with a total projected area normal to the face, should be taken as:

$$F_{m,W}(z) = \frac{q_p(z)}{1+7I_v(z)} \sum c_f A_{ref}$$ **Eq. 2.1**

where:

z is the height above the base at which the load is calculated;

$q_p(z)$ is the peak wind pressure at the effective height according to EN 1991-1-4;

$I_v(z)$ is the turbulence intensity according to EN 1991-1-4/§4.4;

c_f is the wind force coefficient according to EN 1993-3-1/ B.2.2;

A_{ref} is the reference area normal to the face.

The above equation could take the form:

$$F_{m,W}(z) = \frac{1}{2}\rho_{air}v_m^2 \sum c_f A_{ref} = q_m(z) \sum c_f A_{ref}$$ **Eq. 2.2**

where:

v_m is the mean wind velocity according to EN 1991-1-4/§4.3.1;

ρ_{air} is the air density (equal to 1,25Kg/m³).

The mean wind velocity at the height z is:

$$V_m(z) = c_r(z)c_o(z)\left[c_{dir}c_{season}V_{b,0}\right]$$ **Eq. 2.3**

where:

$c_r(z)$ is the roughness coefficient according to EN 1991-1-4/§4.3.2;

$c_o(z)$ is the orography coefficient according to EN 1991-1-4/§4.3.3 and is taken equal to 1,0;

c_{dir} is the directional factor according to EN 1991-1-4/§4.2 and is taken equal to 1,0;

c_{season} is the season factor according to EN 1991-1-4/§4.2 and is taken equal to 1.0;

$v_{b,0}$ is the fundamental value of the basic wind velocity, taken as 25,0m/sec according to the German national annex of EN 1991-1-4 & EN 50341-2-4:2016.

It is assumed that the tower is located in terrain category II, according to EN 50341-2-4:2016, which leads to some characteristic values for the mean wind velocity calculation.

Back Face (43%W)

Front Face (57%W)
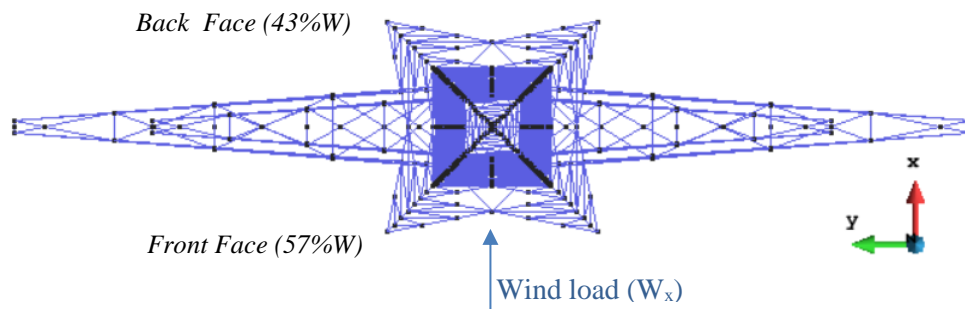
Wind load (W_x)

Figure 2.19: Definition of wind direction

The mean wind loads are calculated for each segment (see Figure 2.2 for the determination of the segments) and for two different wind directions (see Figure 2.19):

- wind loads perpendicular to the cross arms W_x (+X direction);
- wind loads in the direction of the cross arms W_y (+Y direction).

Given that the tower being symmetrical, the directions –X and –Y are the same with +X and +Y respectively (geometry and loads) and they are not considered as a different load case.

Then, the mean wind load in two directions (+X, +Y) is distributed on the front and back face of the tower. The front and back faces are determined each time by the direction of the wind. Specifically, and adopting the same values from the analysis of the telecommunication towers (see chapter 1), for each segment, the front face of the tower (in the wind direction) is supporting 57% of the total wind load and the back face 43% of the total wind load (see Figure 2.19).

Table 2.6 and Table 2.7 summarise the mean wind loads on the tower body and on the cross arms, for two different wind directions (W_x and W_y) and for the two faces of the tower (front and back face).

Table 2.6: Mean wind loads on the tower body for wind perpendicular to the arms (θ=0º)

Part	z_m [m]	$q_m(z)$ [N/m²]	A_{ref} [m²]	$c_{f,s}$ [-]	$F_{m,wx,front}$ [kN]	$F_{m,wx,back}$ [kN]
Segment 1	2,44	213,137	3,21	2,77	1,080	0,815
Segment 2	7,79	359,422	4,07	2,71	2,261	1,706
Segment 3.down-mid	15,20	460,901	6,09	2,97	4,756	3,588
Segment 3.mid-up	24,20	538,936	5,29	2,93	4,769	3,597
Segment 4	30,30	578,843	1,99	2,76	1,810	1,366
Segment 5	35,80	609,375	3,23	2,99	3,358	2,533
Segment 6	40,95	634,548	0,92	2,95	0,983	0,742
Segment 7	46,20	657,574	1,59	2,85	1,694	1,278
Arm 1 (lower arm)	29,77	575,638	6,09	2,74	5,480	4,134
Arm 2 (upper arm)	40,53	632,614	3,51	2,70	3,424	2,583

Table 2.7: Mean wind loads on the tower body for wind in direction with the arms (θ=90°)

Part	z_m [m]	$q_m(z)$ [N/m²]	A_{ref} [m²]	$c_{f,s}$ [-]	$F_{m,wy,front}$ [kN]	$F_{m,wy,back}$ [kN]
Segment 1	2,44	213,137	3,21	2,77	1,080	0,815
Segment 2	7,79	359,422	4,07	2,71	2,261	1,706
Segment 3.down-mid	15,20	460,901	6,09	2,97	4,756	3,588
Segment 3.mid-up	24,20	538,936	5,29	2,93	4,769	3,597
Segment 4	30,30	578,843	0,51	3,61	0,610	0,460
Segment 5	35,80	609,375	3,23	2,99	3,358	2,533
Segment 6	40,95	634,548	0,38	3,51	0,477	0,360
Segment 7	46,20	657,574	1,59	2,85	1,694	1,278
Arm 1 (lower arm)	29,77	575,638	5,74	2,80	5,274	3,978
Arm 2 (upper arm)	40,53	632,614	3,33	2,76	3,310	2,497

At the end, the mean wind load acting on a face is distributed to each bar according to the normal area, to a **constant linear load** along each bar, in order to have a realistic simulation of the wind loads.

B.2 Wind loads on the conductors

The calculation of the wind loads on the conductors is based on EN 1993-3-1/Annex B/B.3.2.2.4. The maximum wind loading on the cables in the direction of wind $F_c(z)$ should be taken as:

$$F_C(z) = \frac{q_p(z)}{1+7I_v(z)} \sum c_{f,G} A_G \left[1 + \frac{[1+7I_v(z)]c_s C_d - 1}{c_o(z)} \right]$$ **Eq. 2.4**

where:

z is the height above the base of the support of the conductor/cable;

$c_{f,G}$ is the wind force coefficient according to EN 1993-3-1/ B.2.3;

A_G is the area normal to the cable;

$c_s c_d$ is the structural factor according to EN 1991-1-4/§6 and is taken equal to 1,0.

Table 2.8 shows the calculation of the wind load on the conductors/earth wire for two different wind directions.

Table 2.8: Wind loads on the conductors

Wind direction	ψ [°]	z [m]	$q_m(z)$ [N/m²]	$C_{f,G,0}$ [-]	$I_v(z)$ [-]	d [mm]	In direction $F_{cy}(z)$ [kN]	Perpendicular $F_{cx}(z)$ [kN]
In direction of the cross arm axis	0	28,70	569,081	1,10	0,157	22,4	20,631	0
		39,70	628,696		0,150		22,212	0
		50,20	673,663		0,145	13,6	7,100	0
Perpendicular to the cross arm axis	90	28,70	569,081	1,10	0,157	22,4	0	0
		39,70	628,696		0,150		0	0
		50,20	673,663		0,145	13,6	0	0

B.3 Wind loads on the insulators

According to EN 1993-3-1/Annex B/B.3.2.2.4, the wind loads on the insulators are these reported in Table 2.9.

Table 2.9: Calculation of wind loads on the insulators

Position of insulator	z [m]	$q_m(z)$ [N/m^2]	$C_{f,G,0}$ [-]	C_c	A_{ins} [m^2]	Each direction
						$F_{ins}(z)$ [kN]
Insulator at the lower arm	28,70	569,081	1,20	1,0	0,150782	0,216
Insulator at the upper arm	39,70	628,696	1,20	1,0	0,150782	0,233

2.4.2 Load combinations

The considered load cases are gravity and wind loads for the tower, the conductors and the insulators. The design actions according to [2] is therefore the following one:

$$E_d = \gamma_G G_K + \gamma_W Q_W$$ **Eq. 2.5**

where:

Ed total loads;

G_K dead loads of conductors, insulators and body of the structure;

Q_W wind forces as specified in EN 1993-3-1.

In each analysis, are considered the following two load combinations with safety load factors. For the determination of the axis, see Figure 2.19.

X direction:

Gravity loads and wind forces perpendicular to the cross arms (W_x).

Y direction:

Gravity loads and wind forces in direction of the cross arms (W_y).

2.4.3 Types of analyses

The safety load factors are adjusted each time according to the analysis. As referred in the introduction, the second main objective of the current report is to validate the initial design of the tower made through the TOWER software. This will be reached by a FINELG full non-linear analysis (to check the design in terms of resistance and stability) after the comparison of the two models in the elastic range. Same safety load factors will be used for the applied loads in those two analyses, in accordance with the safety factors that have been used in the initial design of the tower. Specifically, in case of unfavourable action the safety load factor is $\gamma_G = \gamma_W = 1,35$ according to EN 50341-2-4.

Again as said in the introduction, further studies (elastic instability analyses, elastic second-order analyses) have also been achieved so as to understand better how the structure behaves. Because of some technical difficulties to apply a global safety load factor for an elastic instability analysis in FINELG, the decision has been taken to perform these analyses under un-factored loads. In FINELG software, it is possible, but really time consuming, to apply a global load factor in the instability analysis, in contrast with other types of analysis. So load factors equal to 1,0 will be used. This is not a problem in itself, as the information which is expected from these analyses is independent of the used safety factors.

To summarise, the following analyses will be performed by FINELG:

- a first order linear elastic analysis with safety load factors equal to $\gamma_G = \gamma_W = 1,35$, in order to compare both FINELG and TOWER models;

- an elastic instability analysis with safety load factors equal to 1,0;

- a second-order linear elastic analysis with safety load factors equal to 1,0, to complement the instability analysis;

- Moreover, the previous analyses will be performed with and one without initial imperfections, so as to investigate their influence;
- a second order plastic non-linear analysis with safety load factors equal to 1,0, to evaluate the impact of plasticity on the tower response;

Finally, so as to reach the second main objective of the report, a full non-linear (second-order effects and plasticity) analysis with safety load factors equal to γG = γW = 1,35 will be performed to validate the initial design of the tower made by means of the TOWER software. This analysis will also provide valuable information on the capacity for plastic redistribution in towers.

2.5 Modelling for analyses with FINELG

The modelling of the tower has been done with the FINELG [4] finite element software, using beam elements. FINELG software have been already successfully used in the past, to simulate a lattice tower. Furthermore, the results of this "older" simulation were corresponded to the experimental tests of the tower [11].
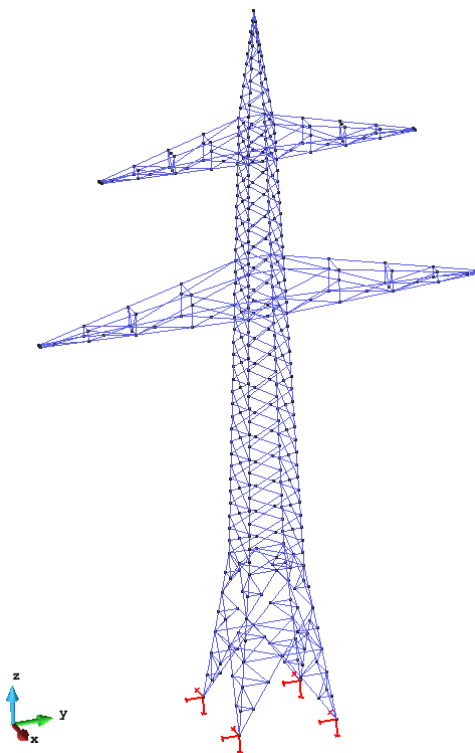
Figure 2.20: 3-D model of the tower with FINELG software

The bolted connections between the different diagonal and leg members as well as the splices of the legs are not considered directly in the model. However, their global response has been simulated through appropriate hinges/constraints at the ends of the elements. Moreover, their self-weight has been considered as referred in 2.4.1 (A1).

The tower structure is modelled using the following assumptions:

- the main legs are modelled considering continuity over their total length;
- the bracing members and horizontal members are considered as pinned at their ends connected to the main legs and to the horizontal members;
- the secondary bracing elements are also considered as pinned at their ends.

The members that are considered as continuity over their total length, are simulated with blocked all the degrees of freedom at their extremities. For the pin-end members, the rotations are free (except the rotation which leads to torsion that is blocked). All the other DOF are blocked too.

Every element/bar is modelled with its appropriate eccentricity, rotation and orientation in order to have a more realistic model. As a result, the elements are not only subjected to axial forces (tension/compression) but also to bending moments, even if they are pin-ended. The foundations are assumed as joined supports.

The conductors have not been modelled. As a result, the wind loads on the conductors and the earth wire as well as their self-weight are calculated apart and entered in the model as point loads acting at the top of the insulators.

2.6 Comparison of FINELG and TOWER models in the elastic range

Before the full non-linear analyses and the validation of the initial design of the tower, it is important to compare the model created by FINELG with the initial model created through the TOWER software. First of all, the self-weight of the structure has been compared to the one provided by TOWER. Then, the maximum displacements for three different load cases have been evaluated, again in view of comparison with TOWER.

As already referred in paragraph 2.3.5, the total weight of the structure reported from TOWER is 16,996 ton = **166, 73kN**. It should be noted that the total weight includes the weight of the angle profiles, the weight of the insulators and the weight of the bolts and gussets which is estimated through a load adjustment factor of 1,2. The corresponding value for total weight load from FINELG software is **172, 60 kN**. The difference between two models is **3, 40**%. In reality, both self-weights should be the same. However, the eccentricity of each bar and its real position, changes slightly the length of the bar, while in TOWER all the members are connected centrally. This small length difference could explain and make acceptable the difference of both self-weights.

Table 2.10: Maximum displacements for linear elastic analysis

Load case	Node with maximum displacement	Direction of displacement	Maximum displacement from TOWER software [m]	Maximum displacement from FINELG software [m]
1,35G	Edge of lower arm	Z	-8,14·10⁻³	-9,61·10⁻³
1,35G+1,35Wₓ	Top of the tower	X	0,301	0,164
1,35G+1,35Wᵧ	Top of the tower	Y	0,514	0,596

The maximum displacements are summarized in Table 2.10. It should be noted that:
- load case 1,35G includes only the self-weight of the tower without the conductors and insulators;
- the wind load calculations being in TOWER and FINELG based on different norms (EN 1993-3-1 for FINELG and EN 50341-1 for TOWER), it is normal to see a difference between those displacements;
- the wind loads in FINELG are introduced as linear loads along the bars while in TOWER they are introduced as loads at the nodes;
- the wind loads on the body of the tower are bigger according to EN 50341-1 than EN 1993-3-1, what justifies the difference in load case $1,35G + 1,35W_x$;
- the wind loads on the conductors are smaller according to EN 50341-1 than EN 1993-3-1, what explain why the difference in load case $1,35G + 1,35W_y$ is smaller than in load case $1,35G + 1,35W_x$.

Regarding those values, one notices that they are high. However:
1. the displacements are appearing at the failure limit state (applying loads with 1,35 load factors) and not at the service limit state (applying loads without load factors);

2. there is no special indication or limitation specified in the norms (EN 1993-3-1 or EN 50341-1) in terms of maximum displacement at service limit state.

The only reason to provide displacements here is to compare the order of magnitude – not even the exact value – between TOWER and FINELG software. However, due to the big difference of the maximum displacements of both software (Table 2.10), complementary analyses have been performed to investigate the stiffness of the two models. In fact, as it has been already said:

- the loads applied in TOWER and FINELG are not exactly the same;
- in TOWER, the elements are considered as connected at the level of their respective centre of gravity axes, while FINELG simulates the eccentricities and the exact orientations of the bars.

So the question is to know where the above-mentioned differences may be assigned to one on the two factors, or to both. Should the differences be only assigned to the loads, one could conclude that the serviceability states can be based on the results of an elastic analysis in which eccentricities and actual position of the members could be ignored, so simplifying drastically the work of the designers.

The comparison of the stiffness evaluated through the TOWER and FINELG models has been achieved through a first order linear elastic analysis. A horizontal load of 1 kN has been applied (i.e. the same loading in TOWER and FINELG) at the top of the tower in the two following situations:

- the load is applied perpendicular to the cross-arm axis (X direction);
- the load is applied in direction of the cross-arm axis (Y direction).

The results are summarized in Table 2.11.

Table 2.11: Displacements on the top of the tower from linear elastic analyses

Load case	Direction of load and displacement	Displacement from TOWER software [m]	Displacement from FINELG software [m]	Difference [%]	Stiffness of FINELG model [kN/m]
F_x=1 kN	X	$9{,}019 \cdot 10^{-3}$	$9{,}455 \cdot 10^{-3}$	4,61	105,76414
F_y=1 kN	Y	$9{,}021 \cdot 10^{-3}$	$9{,}438 \cdot 10^{-3}$	4,42	105,95465

The difference between the displacements is **less than 5%**, what means that both models have almost the same stiffness. This seems to indicate that a simplified modelling of the members at their extremities (as in TOWER) could be accurately contemplated.

2.7 Further investigations on tower's response

In order to understand better the tower response, an elastic instability analysis will be performed and complemented by a second order linear elastic one. Furthermore, a second order plastic analysis will be performed to evaluate the importance of the plasticity effects. For the following analyses, load factors equal to 1,0 will be used. Through those analyses, the influence of the initial imperfections will be also investigated. Finally, the influence of second order effects at the serviceability level will be investigated.

2.7.1 Instability analysis

It is important to notice that "instability analysis" means a first order linear elastic analysis. Specifically, the critical loads have calculated for the load combinations (see paragraph 2.4):

  i. $G + W_x$

  ii. $G + W_y$

The results are summarised in Table 2.12 and in Figure 2.21 and Figure 2.22.

Table 2.12: Results from elastic instability analysis

Load combination	G+W$_x$		G+W$_y$	
No of mode	Load factor λ	Type of instability	Load factor λ	Type of instability
1st	2,270	Member	1,371	Segment
2nd	2,862	Member	1,418	Member
3rd	4,256	Member	1,608	Member
4th	4,279	Segment	1,641	Member
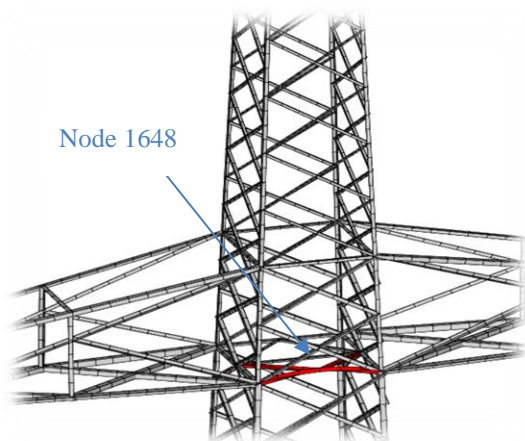
Figure 2.21: First member instability for load combination G+W$_x$
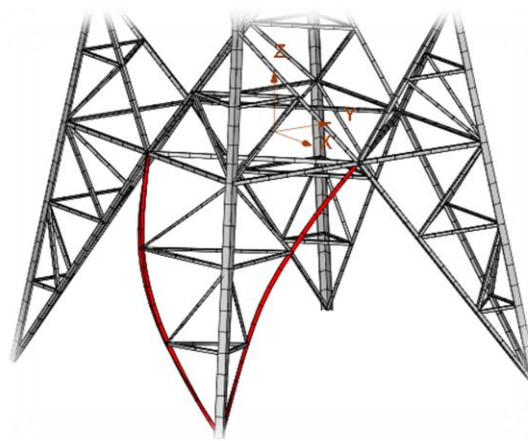
Figure 2.22: First segment instability for load combination G+W$_y$

2.7.2 Non-linear analyses for load combination G+W

Further to the instability analysis of the tower, three complementary analyses have been performed for the same load combination ($G + W$) as previously:

- a geometrically non-linear elastic analysis with elastic material law without initial imperfections;
- a geometrically non-linear elastic analysis with elastic material law considering initial imperfections;
- a geometrically and materially non-linear analysis with full plastic material law (without residual stresses) without initial imperfections.

The initial imperfections have been chosen in accordance with the 1st instability mode, calibrated so as to reach amplitude of L/1000 (L is the length of the member/segment where the instability occurs). The two geometrically non-linear elastic analyses have a double role: to verify the instability analysis and to investigate also the influence of the initial imperfections. Through the third one, has been decided to minimize the parameters (initial imperfections, residual stresses) in order to observe the influence of the plasticity in the structure.

In the analyses, the loads are increased proportionally: $\lambda(G + W)$. The results are summarized, for each direction, in the next paragraphs.

A) $G + W_x$

For the three types of analyses, the failure occurs in the same bar for the vertical displacement u$_z$ (direction of global Z axis - Figure 2.20) at the middle of the bar (node 1648 - see Figure 2.21).

Observing both curves (Figure 2.23), referring to the geometrically non-linear elastic analyses, one concludes that the influence of the initial imperfection on the instability is negligible and the load factor reached for both cases is about $\lambda = 1,62$. Looking to the third curve in Figure 2.23, one sees that the maximum load factor in this case is about $\lambda = 1,52$ and the yielding starts in the same bar too (see Figure 2.24).
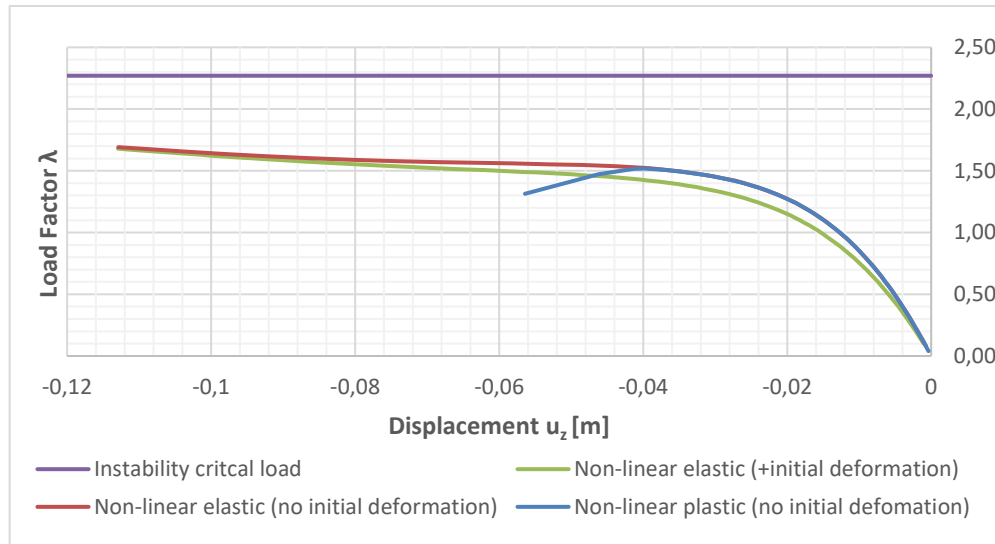
Figure 2.23: Displacement u_z vs LF for different types of analyses - wind perpendicular to the arms (X direction)

It is a priori surprising that the critical load obtained by the instability analysis ($\lambda = 2,27$) is higher than the critical load obtained by the geometrically non-linear elastic analysis ($\lambda \approx 1,62$). If one checks the internal forces at node 1648 for both load factors (see Table 2.13), one realises that the failure occurs for two different triplets of axial force and bending moments (N, M_{by}, M_{bz}). Indeed, in the second order linear elastic analyses, the second order effects are significantly influencing the internal forces in the members. But it is also clear (as investigations on a single angle have shown) bar, that the external forces affect the critical load and may reduce it. At the end, this explains that the "real" critical load is smaller than the load obtained by an instability analysis.
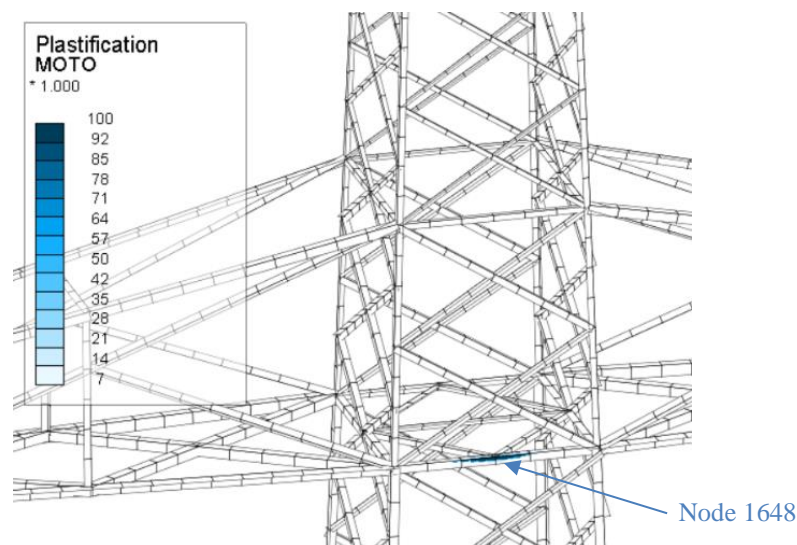
Figure 2.24: Results (plasticisation) from the 2nd order non-linear plastic analysis (X direction)

Table 2.13: Internal forces at node 1648, for the two analyses

Internal forces/Type of analysis	Instability analysis	2nd order linear elastic analysis without initial imperfection
N [kN]	-266,49	-164,10
Torsion M_t [kNm]	0,050	0,368
Bending M_{by} [kNm]	3,557	13,300
Bending M_{bz} [kNm]	-0,24	-10,90
Load factor λ	2,27	1,62

B) $G + W_y$

The behaviour is a bit different for this load combination. First, the failure does not occur only in a certain bar, but in a number of bars, including the critical bar from the first instability mode of the instability analysis. All these bars buckle in X direction, even if the applying wind loads are in Y direction (see Figure 2.20 for the axis). That actually happened due to the eccentricity of those bars, which creates big bending moments and leads the tower to instability. The plasticity starts from a number of lateral bars of the tower: two in the –X one in the +X global direction (front and back side in Figure 2.25). It is easy to observe that the yielding in the backside bar starts simultaneous at the middle and the edges while in the front bar starts in two mid-points.

The graph in Figure 2.26 shows the horizontal displacement u_x (direction of global X axis - Figure 2.20) versus the load factor at the top of the tower. This node has been selected because it represents rather well the global response of the tower. It is again clear from the two curves referring in Figure 2.26 to the non-linear elastic analyses that the influence of the initial imperfection is negligible. The load factor for those cases is about $\lambda = 0,87$. In addition, when material non-linearities are integrated with analysis, the yielding starts from a number of bars and the load factor obtained in this case is about $\lambda = 0,85$. However, it looks like that plastification is leading to a lower ultimate load than the critical one, without the appearance of a plastic mechanism. The difference between the values of the instability analysis and the 2nd order linear elastic analysis could be explained again by the different type of analysis which introduces big bending moments.
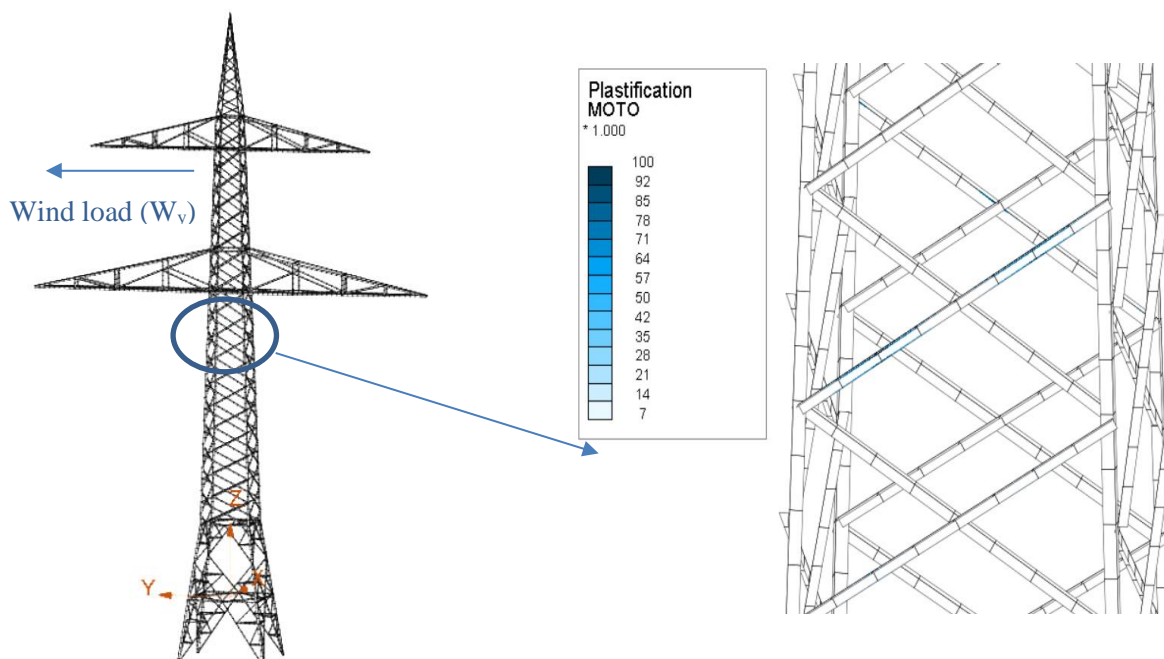
Figure 2.25: Results (plastification) from the 2nd order non-linear plastic analysis (Y direction)
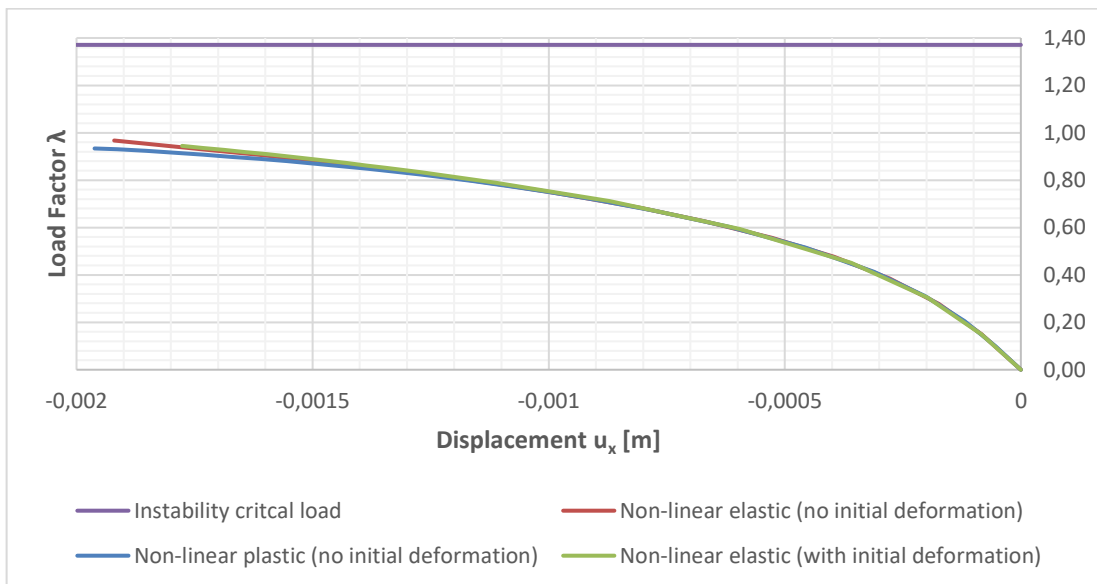
Figure 2.26: Displacement u$_x$ vs LF for different types of analyses - wind in direction of the arms (Y direction)

For the current analyses there were some difficulties of the software to converge, after the points that already represented in the graph. However, is it obvious that even if the software converge to more points, the load factors will not increase, given the fact that the curve is tending to be horizontal.

2.7.3   Influence of the second order effects

A comparison between a first and second order elastic analysis for serviceability loads has been performed with FINELG. Two cases have been considered for those analyses, in which the loads have been applied:

- at the extremities of the tower arms;
- at the top of the tower.

2.7.3.1   Loads at the extremities of the cross arms

In this case, the unfactored gravity loads representing the self-weight of the cables have been applied at the extremities of the cross arms (concentrated loads). Then, a first order linear elastic analysis and a second order linear elastic one with load pattern λG have been performed.

For both cases, the self-weigh of the tower has not been considered. The self-weight calculations of the conductors and insulators are summarized in paragraph 2.4.1.
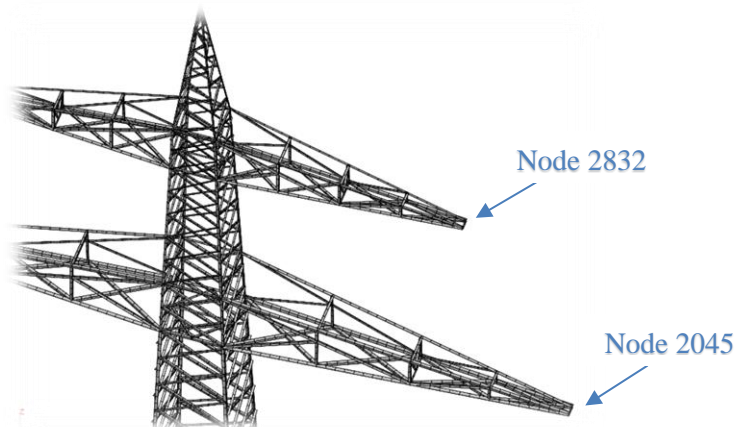
Figure 2.27: Definition of the nodes

Figure 2.28 shows the displacement of nodes 2045 & 2832 (see Figure 2.27) versus the vertical displacement u_z. Observing the different curves, one could realize that the influence of the second order effects is negligible for load factors equal to 1,0, but also smaller than 2,75. For bigger load factors, a member buckling occurs on the tower's body and then the tower becomes unstable.
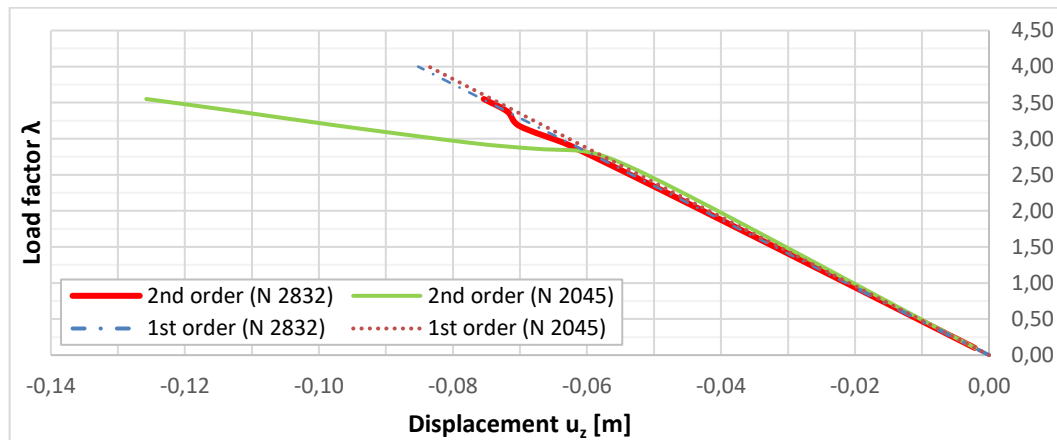
Figure 2.28: Displacement u_z versus load factor for the nodes 2832 and 2045

2.7.3.2 Loads at the top of the tower

For this case, "fictitious" loads have been estimated so as to mimic the reality and reach a displacement equal to the one observed through the full modelling (serviceability load), through a first order linear elastic analysis, at the top of the tower.

Table 2.14: Displacements on the top of the tower from 1st order linear elastic analysis

Direction of load and displacement	Displacement from FINELG software (1st order) [m]	Stiffness of FINELG model [kN/m]	Load case to be performed
X	0,1214	105,76414	F_x=12,842 kN
Y	0,4413	105,95465	F_y=46,759 kN

A) X direction

A load equal to F_x=12,842 kN has been applied at the top of the tower. From Figure 2.30 (left) one sees that the influence of the second order effect on towers response in this direction is negligible since both analyses have given the same results for λ<0,92. However, for a load close to 0,92*12,842=11,81 kN a segment buckling occurs (Figure 2.29) and leads to an instability in Y directions (see Figure 2.30 right).
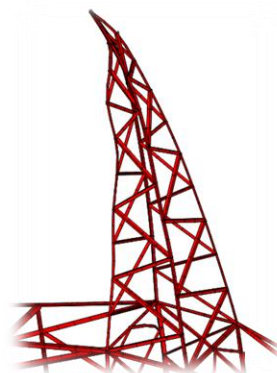
Figure 2.29: Failure (segment buclking) of the tower for the load F_x=12.845kN at the top.
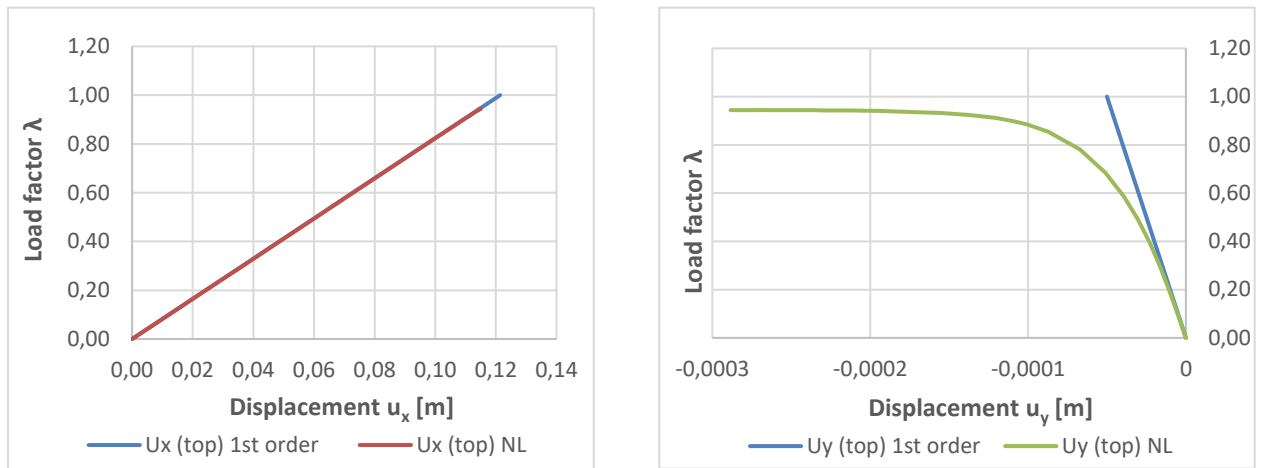
Figure 2.30: Displacements (X left, Y right) of the top of the tower versus LF for different analyses.

B) Y direction

Due to tower's symmetry, the behaviour is exactly this same in this direction. The influence of the second order effect on towers response in the direction of the applying load is negligible and again for a load about 0,236*46,759=11,03 kN, a segment buckling occurs and leads to instability.

As a result, one can conclude that the verification of the serviceability states, if any requirement should be one day specified (what is not the case now), could be achieved on the basis of a first-order elastic analysis. Another conclusion, which should have to be confirmed later in the project, is the fact that even under factored loads, a first-order analysis may be achieved, provided that all instability modes are checked later on through appropriate verification formulae (i.e. in line with the procedure followed by TOWER, except that it has been shown that some failure modes were there nowadays disregarded).

2.8 Validation of the initial design – Full non-linear analysis

At the end, the second main objective of this report is to validate the initial design by TOWER. This will be reached by a full non-linear analysis with FINELG, considering:

- an elastic-perfect plastic material;
- a distribution of residual stresses (Figure 2.14);
- an initial imperfection of the structure in accordance with the 1st instability mode (see 2.7.2).

The load combinations have been described in paragraph 2.4.2. In this case, the gravity loads were fully applied at the beginning and then wind loads applying incrementally $[1,35G + \lambda(1,35W)]$ until failure of the tower occurs. This load sequence simulation is closer to the reality.

Just for comparison, a second-order linear elastic analysis with the same initial imperfection, as the full non-linear, will be performed for this load sequence.

A) $1,35G + 1,35W_x$

As it shown in Figure 2.31, the load factor for the 2nd order linear elastic analysis is about $\lambda \approx 1,62$ while, for the full non-linear analysis it is equal to $\lambda = 1,17$. The failure occurs again at the same bar (node 1648) due to instability or plasticity for the second-order linear elastic analysis and for the full non-linear respectively The graph represents the vertical displacement u_z (direction of global Z axis - Figure 2.20) at the middle of the node 1648 versus the load factor for the design loads for each sequence.

It is important to notice that the load factor for this load combination is bigger than 1,0 with comparison to the design loads. As a result, one could say that the design for this direction is sufficient given the fact that the tower remains in the elastic range for load factors $\lambda \leq 1,0$ and is in accordance with TOWER's design.
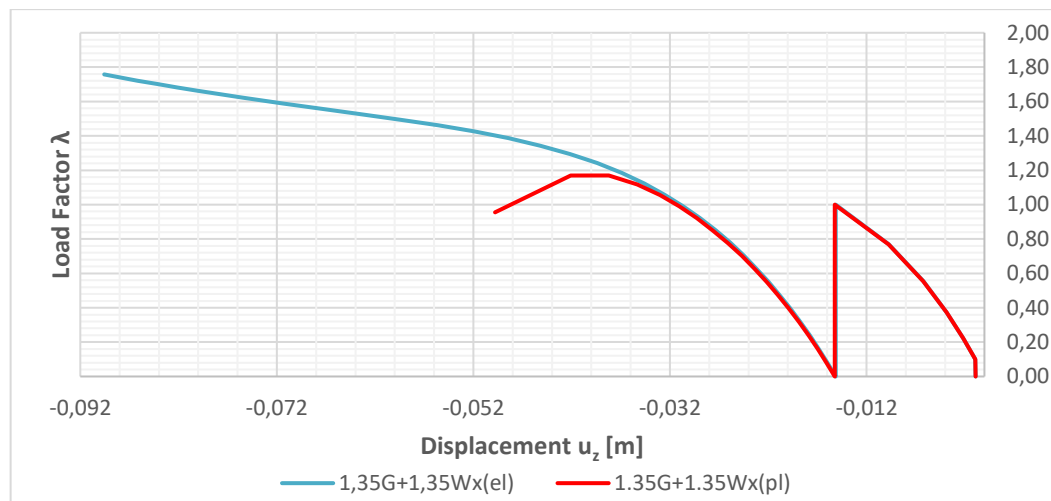

Figure 2.31: Displacement versus LF for different types of analysis – 1.35G+1.35Wx (X direction)

B) $1,35G + 1,35W_y$

Figure 2.32 shows the horizontal displacement u_x (direction of global X axis - Figure 2.20) versus the load factor at the top of the tower. The load factor for the second-order linear elastic analysis is about $\lambda \approx 0,64$ while for the full plastic analysis is about $\lambda \approx 0,62$. It is obvious also for this load sequence that the yielding leads to a lower ultimate load without the appearance of a plastic mechanism.

For those analyses there were some problems again of the software to converge for more points than those have been already present in the graph. However, is it obvious that even if the software would converge for more points, the load factors would never reach a value close or bigger than 1.0, since the curve is almost horizontal.

The design of the tower by TOWER software for this direction may be not sufficient, as the tower did not reach a load factor $\lambda \geq 1,0$ for the design loads.
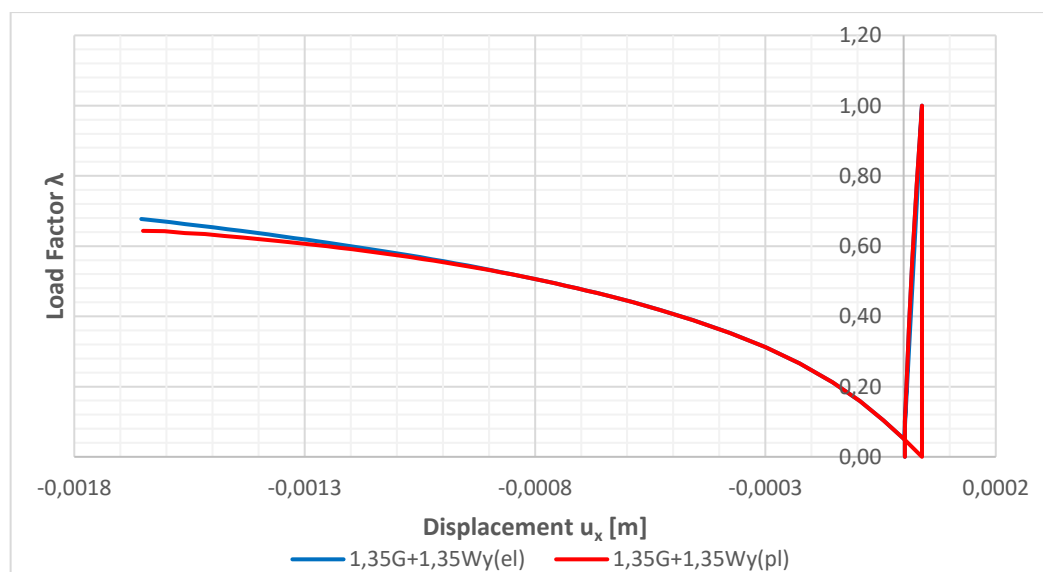
Figure 2.32: Displacement versus LF for different types of analysis – 1.35G+1.35Wy (Y direction)

2.9 Conclusions

From all the results obtained from the different performed analyses, the following conclusions may be drawn:

- There are different norms for the design of transmission towers: EN 1993-3-1 & EN 50341-1.

- Both norms provide different recommendations. In the present report, EN 1993-3-1 has been used for evaluation of the wind loads.

- There is no special indication or limitation in the norms about the maximum displacements of the tower a service limit state. This factor is so not checked, probably because of the lack of specific needs in this regard.

- A reasonable agreement is seen between FINELG and TOWER elastic analyses. The differences may be explained by modelling aspects.

- The "real" critical load obtained by a 2nd order non-linear elastic analysis is smaller than the critical load obtained by a conventional elastic instability analysis. The reason is that the forces acting on the members in both cases differ, so affecting the member buckling load. And these effects are amplified with regard to the actual member support conditions (eccentricities for instance).

- Full non-linear analyses under factored loads have confirmed the lack of influence of the imperfections on the results. The initial design of the tower through the software TOWER appears to be quite unsafe for the application of wind loads in the Y direction. This aspect will have to be further studied but the fact that, in TOWER, all the bars are simulated by truss elements, without any eccentricity, is certainly an important aspect to keep in mind (see bullet point just above). Moreover one could wonder whether this effect is or not covered through the use, in the norms and therefore in TOWER, of reduced buckling length factors for members. Furthermore, in TOWER, the wind loads are applied at the nodes.

2.10 References

[1]   CEN: EN 1993-3-1, Design of steel structures – Part 3-1: Towers, masts and chimneys – Tower and masts, 2006.

[2]   CEN: EN 50341-1, Overhead electrical lines exceeding AC 1 kV - Part 1: General requirements - Common specifications, 2012.

[3]   TOWER User's Manual - Version 15.0, ©Power Line Systems Inc, 2017

[4]   FINELG: Non-linear finite element analysis program, User's manual, Version 9.0, Greisch Ingeniere, 2003

[5]   CEN: EN 50182, Conductors for overhead lines - Round wire concentric lay, 2001.

[6]   Zhang L, Jaspart JP, Stability of members in compression made of large hot-rolled and welded angles, Université de Liège, 2013.

[7]   Reinhard Fischer and Friedrich Kießling: Freileitungen: Planung, Berechnung, Ausführung. 4 Auflage, Springer Verlag, 2013.

[8]   CEN: EN 50341-2-4, Overhead electrical lines exceeding AC 1 kV - Part 2-4: National Normative Aspects (NNA) for Germany (based on EN 50341-1:2012), 2016.

[9]   CEN: EN 1993-1-4, Actions on structures - Part 1-4: General actions, Wind actions, 2005.

[10] CEN: EN 1993-1-1, Design of steel structures - Part 1-1: General rules and rules for buildings, 2005.

[11] Vincent de Ville de Goyet, L'analyse statique non linéaire par la méthode des éléments finis des structures spatiales formées de poutres à section non symétrique, Université de Liège, 1989

3   Lattice girder

3.1   Introduction

This last case study concerns a lattice girder fabricated from back-to-back connected angle sections. The girder is analysed through a linear elastic analysis performed with the commercial software Robot Structural Analysis. In particular, the chosen example highlights the design method that has to be applied to back-to-back connected angle sections whose packing plates are spaced by more than $15i_{min}$.

3.2   Design specifications and other references

Design standards:

[1] **NF EN 1990** (March 2003) – Eurocode : Basis of structural design
[2] **NF EN 1991-1-3** (April 2004) – Eurocode 1 : Actions on structures Part 1-3: General actions – Snow loads
[3] **NF EN 1991-1-3/NA** (May 2007) – Eurocode 1 : Actions on structures Part 1-3: General actions – Snow loads – French National Annex to EN 1991-1-3:2004
[4] **NF EN 1991-1-4** (November 2005) – Eurocode 1 : Actions on structures Part 1-4: General actions – Wind actions
[5] **NF EN 1991-1-4/NA** (March 2008) – Eurocode 1 : Actions on structures Part 1-4: General actions – Wind actions – French National Annex to EN 1991-1-4:2005
[6] **NF EN 1993-1-1** (October 2005) – Eurocode 3 : Design of steel structures - Part 1-1: General rules and rules for buildings

Other references:

[7] Bureau, A., Chouzenoux, P.-L. (2010). Méthode simplifiée pour la vérification de barres comprimées composées de deux cornières assemblées dos-à-dos. Construction Métallique (CTICM), 4.
[8] Delesques, R., (1972). Flambement des barres dont l'effort normal varie sur la longueur. Construction Métallique (CTICM), 4.

3.3   Materials

All elements of the lattice girder are fabricated from steel S275 JR:
  – Yield strength: f_y = 275 MPa
  – Ultimate tensile strength: f_u = 430 MPa
  – Young's modulus: E = 210000 MPa
  – Poisson's ratio: ν = 0,3
  – Density: ρ = 7850 kg/m^3

According to EN 1993-1-1 [6] the yield strength f_y and the ultimate tensile strength f_u may be used for wall thicknesses that are equal to or lower than 40 mm.

3.4   Loads and load combinations

The studied lattice girder supports the roof of an industrial building. Consequently, it is subject to permanent loads resulting from the roof itself and the equipment. Additionally, the studied main girder transfers the climatic loads to the columns. The loads considered for the design in the following are summarised next:

Permanent loads G:

Dead load of the main girder;
Dead load of the purlins: 0,52 kN (applied to all nodes of the upper chord);

Dead load of the roof covering: 3,44 kN (applied to all nodes of the upper chord).

Live loads Q:

Electric installations: 3,75 kN (applied to all nodes of the upper chord);

Ventilation ducts: 4 kN (applied according to Figure 3.1);

Other equipment: 2,75 kN (applied to all nodes of the upper chord).
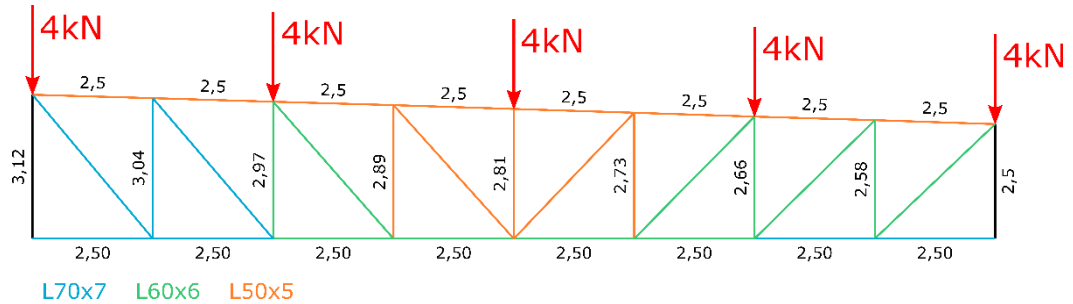
Figure 3.1: Loads resulting from ventilation ducts

Wind loads W:

Wind loads are determined according to EN 1991-1-4 (see references [4] and [5]). The resulting loads are directly given next (the sign "-" indicates suction wind loads):

Longitudinal wind: w = -4,8 kN/m

Transversal wind: w = -4,7 kN/m

As the longitudinal wind yields the higher loads, only the value of -4,8 kN/m is considered when the internal forces are calculated.

Snow loads S:

Snow loads are determined according to EN 1991-1-3 and the French National Annex (see references [2] and [3]). The resulting value is directly given next:

s = 3,4 kN/m

Load combinations:

The loads are combined according to EN 1990 [1]. It should be noted that all live loads Q are considered simultaneously. As the action of the wind only generates suction loads, it is not combined with snow and live loads. The following load combinations are therefore studied:

1) 1,35 G + 1,5 Q + 0,75 S
2) 1,35 G + 1,5 S + 1,05 Q
3) G + 1,5 W

3.5   Geometrical properties

The studied lattice girder, possessing a span of 20 m, corresponds to the rafter of the longitudinal portal frames of the industrial building (in black colour in Figure 3.2). The lattice girder is composed of back-to-back connected angle sections. These angle sections are connected through packing plates that possess a spacing of 50 times the minimum radius of gyration of the angles.

Consequently, the built-up member cannot be treated as single member according to EN 1993-1-1 [6] and the effect of the shear stiffness of the connections has to be accounted for. Figure 3.2 also shows that the lower chord of the lattice girder is restrained against out-of-plane displacements at three points along the span by lacings. The upper chord is restrained in every node of the lattice girder by the purlins (not represented in Figure 3.2).

Longitudinal portal frame (with the studied girder) Jack rafter
Transversal portal frame Lacing
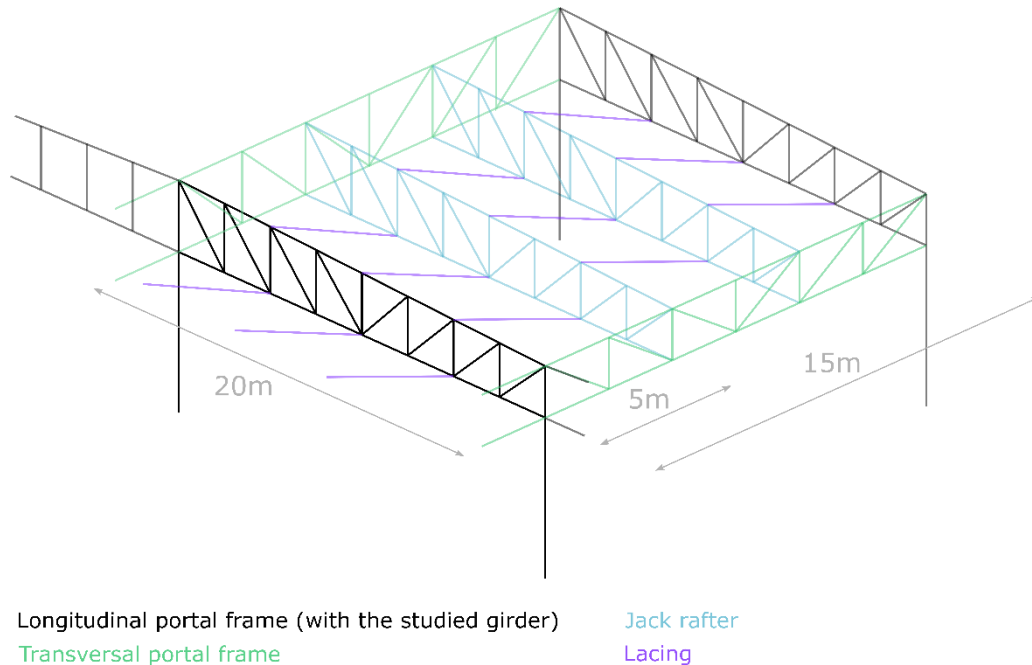
Figure 3.2: Studied lattice girder

Figure 3.3 gives a detailed view of the studied lattice girder. One may observe that three different angle sections are used depending on the position of the built-up members along the lattice girder.
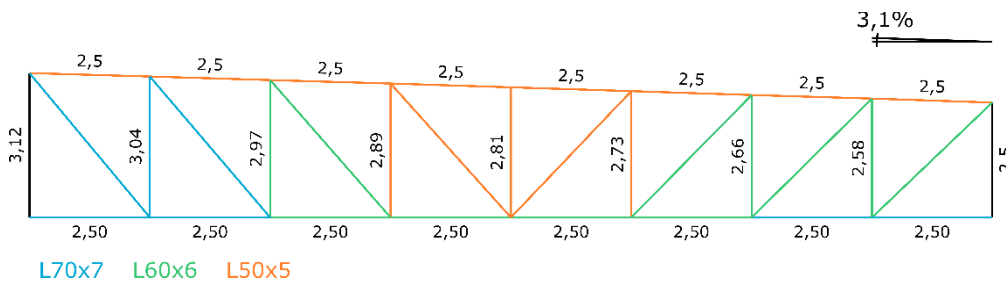
Figure 3.3: Detailed view of lattice girder

3.6 Modelling for analysis

The lattice girder is modelled with the commercial software Robot Structural Analysis. The posts and the diagonals are considered as pinned at their ends. Inversely, the upper and lower chord are considered as continuous. In order to simplify the analysis of the lattice girder, it is extracted from the 3 dimensional numerical model of the industrial building. As the studied lattice girder corresponds to one of the intermediate spans of a multi span portal frame, its ends are considered as clamped in order to represent the effect of the continuity on the internal forces and moments. Therefore, the lattice girder is restrained at the two ends of both chords against vertical and horizontal displacements. The numerical modal of the lattice girder is represented in Figure 3.4.
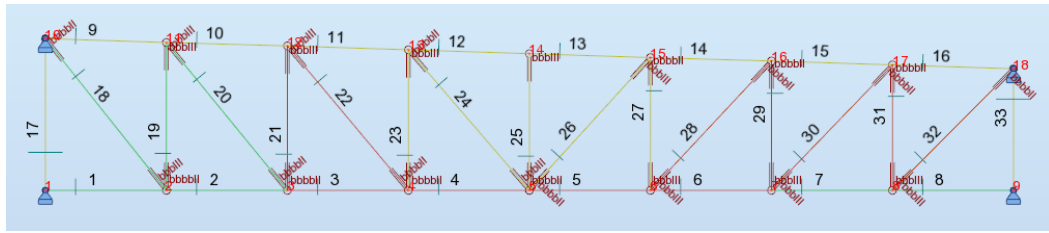
Figure 3.4: Numerical model of the lattice girder

3.7 Structural analysis

The internal forces are determined through first order elastic analyses of the member. Table 3.1 gives the overall maximum values of the internal axial forces. It should be noted that tension forces are considered as negative.

Table 3.1: Summary of axial forces in the members

Member	Maximum compression axial force		Maximum tension axial force	
	Combination	Force (kN)	Combination	Force (kN)
1	2	118,37	3	-54,42
2	2	36,74	3	-17,41
3	3	11,19	2	-26,6
4	3	30,22	2	-66,48
5	3	35,75	2	-77,32
6	3	20,25	2	-44,13
7	2	20,69	3	-8,64
8	2	116,04	3	-52,06
9	3	34,08	2	-77,89
10	3	6,01	2	-14,5
11	2	25,79	3	-12,5
12	2	44,55	3	-20,43
13	2	44,56	3	-19,86
14	2	36,61	3	-16,33
15	2	3,43	3	-0,28
16	3	29,2	2	-61,84
18	3	59,43	2	-130,88
19	2	101,33	3	-47,76
20	3	45,26	2	-100,05
21	2	76,2	3	-35,61
22	3	29,72	2	-62,16
23	2	46,76	3	-23,31
24	3	13,11	2	-28,81
25	2	29,63	3	-13,85
26	3	4,51	2	-11,86
27	2	34,69	3	-17,16
28	3	22,78	2	-48,66

29	2	66,21	3	-30,53
30	3	41,66	2	-93,35
31	2	94,95	3	-44,69
32	3	61,55	2	-135,06

3.8 Structural design

3.8.1 Notations

Before the structural design is performed the notations used hereafter are defined.

a   Spacing of the packing plates
b   Angle leg width
e_0 Amplitude of the built-up element geometric imperfection
h_0 Distance between the angles' centroid
i_v Radius of gyration of the angle section along the minor axis (v-v)
t   Angle leg thickness
t_p Packing plate thickness
u_0 Distance between the shear centre and the centroid of an individual angle section
u'_0 Distance between the shear centre and the centroid of the built-up member

A_{ch} Chord section area
I_{ch} Second moment of area an individual angle section about its z and y axes
$I_{T,ch}$ Torsion constant of an individual angle section
I_T Torsion constant of the built-up member
I_u Second moment of area of an individual angle about the u-u axis (major-axis)
I_v Second moment of area of an individual angle section about the v-v axis (minor-axis)
I_w Warping constant of an individual angle section
$I_{y'}$ Second moment of area of the built-up member about the y'-y' axis
$I_{z'}$ Second moment of area of the built-up member about the z'-z' axis
L   Total length
S_v Shear stiffness of the built-up element
$W_{el,u}$ Elastic modulus of an angle about its major axis
$W_{el,v}$ Elastic modulus of an angle about its minor axis

The axes referred to during the structural design are defined in Figure 3.5 and Figure 3.6 for the built-up member and the individual angle section, respectively.
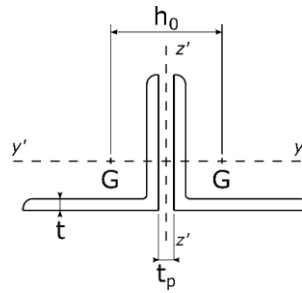
Figure 3.5: Definition of axis for the built-up member
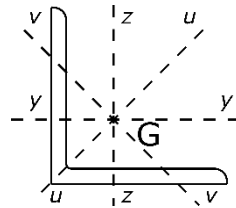
Figure 3.6: Definition of axis for the individual angle section

3.8.2   General

It is recalled that the spacing of the packing plates connecting the chords of the built-up member is greater than 15 times the minimum radius of gyration of the individual angle section. According to EN 1993-1-1 [6], it is therefore not possible to consider the member as a single integral member. Consequently, the design procedure proposed in EN 1993-1-1 [6] for battened compression members is applied hereafter (§6.4.3). As this method is rather lengthy, it is only detailed for the member marked in Figure 3.7 (noted as member 1-2 in the following). This figure also represents the restraints against out-of-plane displacements (represented as black crosses). It is recalled that the restraints result from the purlins for the upper chord and the lacings for the lower chord (see Figure 3.2).
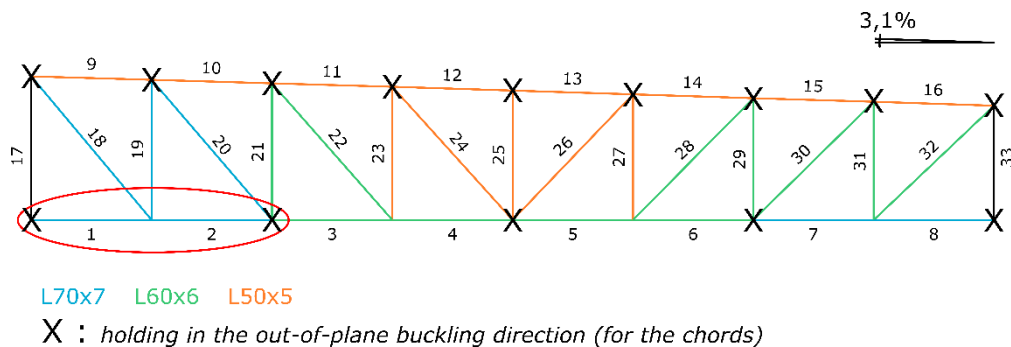
Figure 3.7: Built-up member studied explicitly

The studied member 1-2 is subjected to a stepwise constant axial force. As shown in Table 3.1, the axial force attains 118,37 kN in the first segment of the member (segment noted as 1 in Figure 3.7) whereas it attains only 36,74 kN in its second segment (segment noted as 2 in Figure 3.7). The variation of the axial force is considered for the calculation of the critical axial force for out-of-plane buckling according to the method proposed in reference [8].

3.8.3   Detailed design steps

Before the design steps are detailed, the cross-section properties of the studied member are given in Table 3.2.

Table 3.2: Cross section characteristics of member 1-2

Cross-section properties

Individual angle section	Area:	$A = 9,40$ cm²
	Section modulus about the u-axis:	$W_{el,u} = 13,57$ cm³
	Section moduli about the v-axis:	$W_{el,v,min} = 6,24$ cm³ $W_{el,v,max} = 7,05$ cm³
	Second moment of area about the y- and z-axes:	$I_y = I_z = I_{ch} = 42,30$ cm⁴
	Second moment of area about the u-axis (major axis):	$I_u = 67,19$ cm⁴
	Second moment of area about the v-axis (minor axis):	$I_v = 17,41$ cm⁴
	Torsion constant:	$I_{T,ch} = 1,60$ cm⁴
	Distance between the shear centre and the centroid along the u-axis:	$u_0 = 2,11$ cm
Built-up member	Area:	$A = 18,80$ cm²
	Second moment of area about the y' axis:	$I_{y'} = 84,60$ cm⁴
	Second moment of area about the z' axis:	$I_{z'} = 190,20$ cm⁴
	Torsion constant:	$I_T = 3,20$ cm⁴
	Distance between the shear centre and the centroid along the z'-axis:	$u'_0 = 1,97$ cm
	Distance between the angles' centroids:	$h_0 = 1,97$ cm

First, the resistance of member 1-2 with respect to in-plan buckling (buckling about the y'-y' axis) is checked. The member is restrained against in-plane displacements at mid-span by the post and the diagonal. Therefore its buckling length is equal to 2,5 m. The design steps associated with in-plane buckling are summarised in Table 3.3.

Table 3.3: Design steps for in-plane buckling of the built-up member

Step	Equation	Result
Critical axial force for in-plane buckling	$$N_{cr,y'} = \frac{\pi^2 \, E \, I_{y'}}{L_{cr,y'}^{\,2}}$$	$N_{cr,y'} = 280{,}55 \, kN$
Relative slenderness for in-plane buckling	$$\bar{\lambda}_{y'} = \sqrt{\frac{2A_{ch} \, f_y}{N_{cr,y'}}}$$	$\bar{\lambda}_{y'} = 1{,}36$
Buckling curve	-	b: α = 0,34
Coefficient Φ	$\Phi = 0{,}5 \left[1 + 0{,}34(\bar{\lambda} - 0{,}2) + \bar{\lambda}^2\right]$	$\Phi = 1{,}62$
Reduction factor	$$\chi = \frac{1}{\Phi + \sqrt{\Phi^2 - \bar{\lambda}^2}}$$	$\chi = 0{,}400$
Design criterion	$$\Gamma_{b,Rd} = \frac{N_{Ed}}{\chi \, 2A_{ch} \, f_y / \gamma_{M1}}$$	$\Gamma_{b,Rd} = 0{,}64$

Next, the resistance of the built-up member with respect to out-of-plane instability is checked. As the distance between the packing plates (= 50i_{min}) exceeds the limit of 15i_{min} defined in EN 1993-1-1 [6] for the treatment of the built-up member as a whole, it is necessary to consider the effect of the shear stiffness of the connections between the chords in the design. Here, the procedure proposed in EN 1993-1-1 [6] for battened columns is applied (see also reference [7]). It should be noted that a distance of 50i_{min} between the packing plates corresponds to a practical habit in Europe.

The preparatory design steps are summarised in Table 3.4. In particular, this table gives the details for the determination of the internal forces and moments acting in a single chord based on the assumption that the built-up member acts as a battened column.

Table 3.4: Design steps for out-of-plane buckling of the built-up member – General part

Step	Equation	Result
Equivalent geometric imperfection	$$e_0 = L/500$$	$e_0 = 1cm$
Geometric slenderness of the built-up member	$$\lambda = \frac{L_{cr,z'}}{i_0}$$	$\lambda = 129{,}33$
Coefficient μ	$\mu = 2 - \lambda/75$	$\mu = 0{,}276$
Effective second moment of area of the built-up member	$I_{eff} = 0{,}5 \, h_0^{\,2} \, A_{ch} + 2 \, \mu \, I_{ch}$	$I_{eff} = 128{,}91 \, cm^4$
Critical axial force for minor axis buckling	$$N_{cr} = \frac{\pi^2 \, E \, I_{eff}}{L_{cr,z'}^{\,2}}$$	$N_{cr} = 157{,}89 \, kN$
Shear stiffness of the built-up member	$$S_v = \frac{2\pi^2 \, E \, I_{ch}}{a^2}$$	$S_v = 3792{,}03 \, kN$
Maximum bending moment along the built-up member at mid-span including second order effects	$$M_{Ed} = \frac{N_{Ed} \, e_0}{1 - N_{Ed}/N_{cr} - N_{Ed}/S_v}$$	$M_{Ed} = 5{,}40 \, kN.m$

Maximum axial force in a chord	$N_{ch,Ed} = 0,5\,N_{Ed} + \dfrac{M_{Ed}\,h_0\,A_{ch}}{2\,I_{eff}}$	$N_{ch,Ed} = 152,56\ kN$
Maximum shear force in the built-up member	$V_{Ed} = \dfrac{\pi\,M_{Ed}}{L}$	$V_{Ed} = 3,40\ kN$
Vierendeel bending moment in a chord (about the z'-z' axis)	$M_{ch,Ed} = \dfrac{V_{Ed}\,a}{4}$	$M_{ch,Ed} = 0,58\ kN.m$
Resulting bending moment about the angle's u-u axis	$M_{u,Ed} = M_{ch,Ed}\cos(45°)$	$M_{u,Ed} = 0,41\ kN.m$
Resulting bending moment about the angle's v-v axis	$M_{v,Ed} = M_{ch,Ed}\cos(45°)$	$M_{v,Ed} = 0,41\ kN.m$

Next, the resistance of the individual chord is checked based on the internal forces and moments $N_{ch,Ed}$, $M_{u,Ed}$ and $M_{v,Ed}$. As the chord is subject to compression and bi-axial bending, the interaction equations (6.61) and (6.62) are applied together with Annex A of EN 1993-1-1 (for the determination of the interaction coefficients). Before the resistance of the chord is checked with respect to interaction between buckling and lateral torsional buckling, it is necessary to check the cross-section resistance at the member ends.

It yields:

$$\Gamma_\sigma = \frac{N_{ch,Ed}}{A_{ch}\,{f_y}/{\gamma_{M0}}} + \frac{M_{u,Ed}}{W_{el,u}\,{f_y}/{\gamma_{M0}}} + \frac{M_{v,Ed}}{W_{el,v}\,{f_y}/{\gamma_{M0}}} = 0,91$$

Then, Table 3.5 summarises the verification of the resistance of the chord with respect to flexural torsional buckling.

Table 3.5: Design steps for flexural torsional buckling of the chord

Step	Equation	Result
Chord's critical axial force for buckling about its major axis	$N_{cr,u} = \dfrac{\pi^2\,E\,I_u}{a^2}$	$N_{cr,u} = 3012\ kN$
Chord's critical axial force for torsional buckling	$N_{cr,T} = \dfrac{A_{ch}}{I_0}\left(G\,I_{T,ch}\right)$	$N_{cr,T} = 961\ kN$
Chord's critical axial force for flexural torsional buckling	$N_{cr,TF}$ $= \dfrac{I_0}{2(I_u + I_v)}\left[N_{cr,u} + N_{cr,T} \right.$ $\left. - \sqrt{\left(N_{cr,u} + N_{cr,T}\right)^2 - 4\,N_{cr,u}\,N_{cr,T}\dfrac{I_u + I_v}{I_0}}\right]$	$N_{cr,TF} = 851\ kN$
Relative slenderness for flexural torsional buckling	$\bar{\lambda}_{TF} = 0,55$	$\bar{\lambda}_{TF} = 0,55$

Buckling curve	-	b: $\alpha = 0,34$
Coefficient ϕ	$\phi = 0,5 \left[1 + 0,34(\bar{\lambda}_{TF} - 0,2) + \bar{\lambda}_{TF}^2 \right]$	$\phi = 0,71$
Reduction factor for flexural torsional buckling	$\chi_{TF} = \dfrac{1}{\phi + \sqrt{\phi^2 - \bar{\lambda}_{TF}^2}}$	$\chi_{TF} = 0,86$
Resistance of the chord with respect to flexural torsional buckling	$N_{b,TF,Rd} = \chi_{TF} \, A_{ch} \, f_y / \gamma_{M1}$	$N_{b,TF,Rd} = 222 \; kN$
Design criterion	$\Gamma_{b,TF,Rd} = \dfrac{N_{ch,Ed}}{N_{b,TF,Rd}}$	$\Gamma_{b,TF,Rd} = 0,69$

Table 3.6 gives the details of the design procedure applied to check the resistance of the chord with respect to minor-axis flexural buckling.

Table 3.6: Design steps for buckling about the chord's minor axis

Chord's critical axial force for buckling about its minor axis	$N_{cr,v} = \dfrac{\pi^2 \, E \, I_v}{a^2} = 780 \; kN$	$N_{cr,v} = 780 \; kN$
Relative slenderness for minor axis flexural buckling	$\bar{\lambda}_v = \sqrt{\dfrac{A_{ch} \, f_y}{N_{cr,v}}}$	$\bar{\lambda}_v = 0,58$
Buckling curve	-	b: $\alpha = 0,34$
Coefficient ϕ	$\phi = 0,5 \left[1 + 0,34(\bar{\lambda}_v - 0,2) + \bar{\lambda}_v^2 \right]$	$\phi = 0,73$
Reduction factor for minor axis flexural buckling	$\chi_v = \dfrac{1}{\phi + \sqrt{\phi^2 - \bar{\lambda}_v^2}}$	$\chi_v = 0,85$
Resistance of the chord with respect to minor axis flexural buckling	$N_{b,v,Rd} = \chi_v \, A_{ch} \, f_y / \gamma_{M1}$	$N_{b,v,Rd} = 219 \; kN$
Design criterion	$\Gamma_{b,v,Rd} = \dfrac{N_{ch,Ed}}{N_{b,v,Rd}}$	$\Gamma_{b,v,Rd} = 0,70$

As the angle section is subject to major axis bending, its resistance with respect to lateral torsional buckling should be checked. For this design criterion paragraph 6.3.2.2 of EN 1993-1-1 [6] is applied. The procedure is summarised in Table 3.7.

Table 3.7: Design steps for lateral torsional buckling of the chord

Chord's critical bending moment	$M_{cr} = C_1 \dfrac{\pi^2 E I_v}{a^2} \sqrt{\dfrac{a^2 G I_T}{\pi^2 E I_v}}$ With $C_1 = 2{,}55$	$M_{cr} = 81 kN.m$
Relative slenderness for lateral torsional buckling	$\bar{\lambda}_{LT} = \sqrt{\dfrac{W_{el,u} f_y}{M_{cr}}}$	$\bar{\lambda}_{LT} = 0{,}21$
Buckling curve	-	d: $\alpha = 0{,}76$
Coefficient ϕ	$\phi = 0{,}5 \left[1 + 0{,}76(\bar{\lambda}_{LT} - 0{,}2) + \bar{\lambda}_{LT}^{\ 2}\right]$	$\phi = 0{,}53$
Reduction factor for lateral torsional buckling	$\chi_{LT} = \dfrac{1}{\phi + \sqrt{\phi^2 - \bar{\lambda}_{LT}^{\ 2}}}$	$\chi_{LT} = 0{,}99$
Resistance of the chord with respect to lateral torsional buckling	$M_{b,Rd} = \chi_{LT} W_{el,u} f_y/\gamma_{M1}$	$M_{b,Rd} = 3{,}69 \, kN.m$
Design criterion	$\Gamma_{LTB,ch} = \dfrac{M_{u,Ed}}{N_{b,v,Rd}}$	$\Gamma_{LTB,ch} = 0{,}11$

Up to this point, the resistance of the chord has been checked with respect to the instability modes of flexural buckling, flexural torsional buckling and lateral torsional buckling. Hereafter, the interaction between the modes is addressed by the application of the interaction equations (6.61) and (6.62) of EN 1993-1-1 [6]. It is recalled that Annex A of this standard is used for the determination of the interaction factors. Table 3.8 summarises the different design steps.

Table 3.8: Design steps for lateral torsional buckling of the chord

Equivalent uniform moment factor for major axis bending	$C_{mu,0} = 0{,}79 - 0{,}21\psi + 0{,}36(1 - \psi)\dfrac{N_{Ed}}{N_{cr,u}}$ With $\psi = -1$	$C_{mu,0} = 0{,}56$
Equivalent uniform moment factor for minor axis bending	$C_{mv,0} = 0{,}79 - 0{,}21\psi + 0{,}36(1 - \psi)\dfrac{N_{Ed}}{N_{cr,v}}$ With $\psi = -1$	$C_{mv,0} = 0{,}49$
Limit slenderness $\bar{\lambda}_{0,lim}$	$\bar{\lambda}_{0,lim} = 0{,}2\sqrt{C_1} \sqrt[4]{\left(1 - \dfrac{N_{ch,Ed}}{N_{cr,v}}\right)\left(1 - \dfrac{N_{ch,Ed}}{N_{cr,TF}}\right)}$	$\bar{\lambda}_{0,lim} = 0{,}29$
Slenderness $\bar{\lambda}_0$ of the chord	$\bar{\lambda}_0 = \sqrt{C_1}\bar{\lambda}_{LT}$	$\bar{\lambda}_0 = 0{,}34$
As the slenderness $\bar{\lambda}_0$ of the chord exceeds the limit slenderness, it is necessary to determine a modified equivalent uniform moment factor C_{mu} and the equivalent uniform moment factor C_{mLT}		
Coefficient a_{LT}	$a_{LT} = 1 - I_T/I_u$	$a_{LT} = 0{,}98$

Coefficient ε_u	$$\varepsilon_u = \frac{M_{u,Ed}\, A_{ch}}{N_{ch,Ed}\, W_{el,u}}$$	$\varepsilon_u = 0{,}19$
Resulting equivalent uniform moment factor C_{mu}	$$C_{mu} = C_{mu,0} + \left(1 - C_{mu,0}\right)\frac{\sqrt{\varepsilon_u}\, a_{LT}}{1 + \sqrt{\varepsilon_u}\, a_{LT}}$$	$C_{mu} = 0{,}69$
Resulting equivalent uniform moment factor C_{mv}	$$C_{mv} = C_{mv,0}$$	$C_{mv} = 0{,}49$
Equivalent uniform moment factor C_{mLT}	$$C_{mLT} = C_{mu}{}^2 \frac{a_{LT}}{\sqrt{\left(1 - \frac{N_{ch,Ed}}{N_{cr,v}}\right)\left(1 - \frac{N_{ch,Ed}}{N_{cr,T}}\right)}}$$ $$\geq 1{,}0$$	$C_{mLT} = 0{,}56$ As C_{mLT} is less than 1, the value of 1,0 should be considered $C_{mLT} = 1{,}0$
Coefficient μ_u	$$\mu_u = \frac{1 - \frac{N_{ch,Ed}}{N_{cr,u}}}{1 - \chi_u \frac{N_{ch,Ed}}{N_{cr,u}}}$$	$\mu_u = 1{,}0$
Coefficient μ_v	$$\mu_v = \frac{1 - \frac{N_{ch,Ed}}{N_{cr,v}}}{1 - \chi_v \frac{N_{ch,Ed}}{N_{cr,v}}}$$	$\mu_v = 0{,}97$
Interaction factor k_{uu}	$$k_{uu} = C_{mu} C_{mLT} \frac{\mu_u}{1 - \frac{N_{ch,Ed}}{N_{cr,u}}}$$	$k_{uu} = 0{,}72$
Interaction factor k_{vu}	$$k_{vu} = C_{mu} C_{mLT} \frac{\mu_v}{1 - \frac{N_{ch,Ed}}{N_{cr,u}}}$$	$k_{vu} = 0{,}70$
Interaction factor k_{vv}	$$k_{vv} = C_{mv} \frac{\mu_v}{1 - \frac{N_{ch,Ed}}{N_{cr,v}}}$$	$k_{vv} = 0{,}58$
Interaction factor k_{uv}	$$k_{uv} = C_{mv} \frac{\mu_u}{1 - \frac{N_{ch,Ed}}{N_{cr,v}}}$$	$k_{uv} = 0{,}60$
Design criterion (6.61)	$$\Gamma_{6.61} = \frac{N_{ch,Ed}}{N_{b,u,Rd}} + k_{uu}\frac{M_{u,Ed}}{M_{b,Rd}}$$ $$+ k_{uv}\frac{M_{v,Ed}}{W_{el,v,min}\, f_y/\gamma_{M1}}$$	$\Gamma_{6.61} = 0{,}81$
Design criterion (6.62)	$$\Gamma_{6.62} = \frac{N_{ch,Ed}}{N_{b,v,Rd}} + k_{vu}\frac{M_{u,Ed}}{M_{b,Rd}}$$ $$+ k_{vv}\frac{M_{v,Ed}}{W_{el,v,min}\, f_y/\gamma_{M1}}$$	$\Gamma_{6.62} = 0{,}90$

The chosen member satisfies all design criteria. The design steps for the other members are not detailed hereafter. Rather, a synthesis of the most critical design criteria is provided in the next paragraph.

3.8.4 Synthesis of design checks

Last, Table 3.9 summarises the results of the design checks for all members. One may note, that only the most critical design criterion is specified. The notations used in Table 3.9 are recalled hereafter:

Γ_σ: Cross section resistance at the end of the individual angle section acting as chord of the built-up member;

$\Gamma_{6.62}$: Interaction between lateral torsional buckling and buckling about the v'-axis for the individual angle section acting as chord of the built-up member (design criterion (6.62) of EN 1993-1-1);

$\Gamma_{b,y'}$: Buckling of the built-up member about its minor axis (y'-axis).

Table 3.9: Synthesis of design checks

Member	$N_{Ed,max}$ (kN)	Member length (m)	Cross section	Packing plate thickness (mm)	Resistance criterion	
1	118,37	2,50	L70x70x7	8	Γ_σ =	0,91
2	36,74	2,50				
3	11,19	2,50	L60x60x6	6	$\Gamma_{b,y'}$ =	0,25
4	30,22	2,50				
5	35,75	2,50	L60x60x6	6	$\Gamma_{6.62}$ =	0,32
6	20,25	2,50				
7	20,69	2,50	L70x70x7	8	$\Gamma_{6.62}$ =	0,65
8	116,04	2,50				
9	34,08	2,50	L50x50x5	6	$\Gamma_{b,y'}$ =	0,57
10	6,01	2,50	L50x50x5	6	$\Gamma_{b,y'}$ =	0,10
11	25,79	2,50	L50x50x5	6	$\Gamma_{b,y'}$ =	0,43
12	44,55	2,50	L50x50x5	6	$\Gamma_{b,y'}$ =	0,74
13	44,56	2,50	L50x50x5	6	$\Gamma_{b,y'}$ =	0,74
14	36,61	2,50	L50x50x5	6	$\Gamma_{b,y'}$ =	0,61
15	3,43	2,50	L50x50x5	6	$\Gamma_{b,y'}$ =	0,06
16	29,20	2,50	L50x50x5	6	$\Gamma_{b,y'}$ =	0,48
18	59,43	4,00	L70x70x7	8	$\Gamma_{b,y'}$ =	0,64
19	101,33	3,04	L70x70x7	8	$\Gamma_{b,y'}$ =	0,67
20	45,26	3,94	L70x70x7	8	$\Gamma_{b,y'}$ =	0,47
21	76,20	2,97	L60x60x6	6	$\Gamma_{b,y'}$ =	0,86
22	29,72	3,88	L60x60x6	6	$\Gamma_{b,y'}$ =	0,54
23	46,76	2,89	L50x50x5	6	$\Gamma_{b,y'}$ =	1,00
24	13,11	3,82	L50x50x5	6	$\Gamma_{b,y'}$ =	0,47

25	29,63	2,81	L50x50x5	6	$\Gamma_{b,y'}$ =	0,61
26	4,51	3,70	L50x50x5	6	$\Gamma_{b,y'}$ =	0,15
27	34,69	2,73	L50x50x5	6	$\Gamma_{b,y'}$ =	0,67
28	22,78	3,65	L60x60x6	6	$\Gamma_{b,y'}$ =	0,37
29	66,21	2,66	L60x60x6	6	$\Gamma_{b,y'}$ =	0,62
30	41,66	3,59	L60x60x6	6	$\Gamma_{b,y'}$ =	0,66
31	94,95	2,58	L60x60x6	6	$\Gamma_{b,y'}$ =	0,84
32	61,55	3,53	L60x60x6	6	$\Gamma_{b,y'}$ =	0,95

3.9   Conclusions

This chapter addressed the design of a typical lattice girder used in industrial buildings. The lattice girder is fabricated from back-to-back connected angle sections. These built-up members may fail by buckling about their minor axis (noted as y'-axis throughout this report) or by buckling about their major axis (noted as z'-axis throughout this report). If the buckling lengths about the axes of the built-up member are identical, buckling about their minor axis is obviously the critical failure mode. Nonetheless, in case of lattice girders, especially the upper and lower chord may possess different buckling lengths about their two main axes as the out-of-plane restraints are not always applied at every node of the lattice girder. In this case buckling about the major axis may become relevant. If the distance between the packing plates is less than a certain limit defined in EN 1993-1-1 [6] for back-to-back connected and star battened sections ($15i_{min}$ for back-to-back connected angle sections) the built-up member can be treated as a whole without considering the effect of the shear stiffness of the packing plates. Consequently, the design approach is simple. However, in practice, the distance between the packing plates often exceeds the defined limit and the shear stiffness has to be accounted for during the design of the built-up member leading to a complexification of the design. Additionally, the design approach to be applied, i.e. Eurocode 3 method used for battened columns together with the interaction equations (6.61) and (6.62) (see reference [6]), has not been developed for closely spaced built-up members. Consequently, the precision of the design approach is doubtful. Therefore, the behaviour of closely spaced built-up members is studied further on in Work Package 3 of the ANGELHY project based on laboratory tests and numerical simulations.

List of Figures

List of Tables